#5 and #v integrins cooperate to regulate vascular smooth muscle and neural crest functions in vivo

Citation: Turner, C. J., K. Badu-Nkansah, D. Crowley, A. van der Flier, and R. O. Hynes. "α5 and αv Integrins Cooperate to Regulate Vascular Smooth Muscle and Neural Crest Functions in Vivo." Development 142, no. 4 (February 10, 2015): 797–808.

As Published: http://dx.doi.org/10.1242/dev.117572

Publisher: Company of Biologists

Persistent URL: http://hdl.handle.net/1721.1/98137

Version: Author's final manuscript: final author's manuscript post peer review, without publisher's formatting or copy editing

α5 and αv integrins cooperate to regulate vascular smooth muscle and neural crest functions in vivo.

Christopher Turner, Kwabena Badu-Nkansah, Denise Crowley, Arjan van der Flier and Richard O. Hynes

Howard Hughes Medical Institute, Koch Institute for Integrative Cancer Research,

Massachusetts Institute of Technology, Cambridge, MA 02139, USA

Correspondence: Richard Hynes

Massachusetts Institute of Technology

Cambridge, MA 02139

Tel: 617-253-6422

Fax: 617-253-8357

Email: rohynes@mit.edu

Abstract

The RGD-binding α5 and αv integrins have been shown to be key regulators of vascular smooth muscle cell (vSMC) function in vitro. However, their role on vSMCs during vascular development in vivo remains unclear. To address this issue, we have generated mice that lack α5, αv or both α5 and αv integrins on their vSMCs using the *SM22α-Cre* transgenic mouse line. To our surprise, neither α5 nor αv mutants displayed any obvious vascular defects during embryonic development. In contrast, mice lacking both α5 and αv integrins developed interrupted aortic arches, large brachiocephalic/carotid artery aneurysms, and cardiac septation defects, but developed extensive and apparently normal vasculature in the skin. Cardiovascular defects were also found, along with cleft palate and ectopically located thymi, in *Wnt1-Cre* α5/αv mutants, suggesting that α5 and αv cooperate on neural crest-derived cells to control the remodeling of the pharyngeal arches and septation of the heart and outflow tract. Analysis of cultured α5/αv-deficient vSMCs suggests this is achieved, at least in part, through proper assembly of RGD-containing extracellular matrix (ECM) proteins and the correct incorporation and activation of latent TGF-β.

Introduction

Vascular smooth muscle cells (vSMCs) are specialised cells found wrapped around arteries, arterioles, and large veins. Most vSMCs are derived from the mesoderm (Mikawa and Gourdie, 1996; Wasteson et al., 2008), however vSMCs surrounding the ascending aorta and aortic arch are derived from the neural crest (Jiang et al., 2000), while vSMCs at the aortic root originate from the secondary heart field (Waldo et al., 2005). During development, a major function of vSMCs is to synthesise and assemble large quantities of extracellular matrix (ECM) around newly formed vessels to provide the vasculature with elasticity and structural strength to withstand the pulsatile blood flow from the heart. The ECM deposited around the vasculature has many functions beyond this structural role however (Hynes, 2009). Previous studies have shown that the ECM within the vessel wall regulates the attachment, contractility, motility, proliferation and differentiation of vSMCs (Raines, 2000). Furthermore, its now clear that the ECM plays an important role in the patterning and development of the vascular system by binding to, and regulating the availability and activity of, numerous growth factors and morphogens.

The interaction of transforming growth factor-beta (TGF-β) with the ECM in particular appears essential for regulating cardiovascular morphogenesis and function (ten Dijke and Arthur, 2007; Horiguchi et al., 2012). TGF-β is synthesised as an inactive complex bound to a latent associated protein (LAP) and is incorporated into the ECM through covalently binding to latent TGF-β-binding proteins (specifically LTBP-1, -3 and -4) that interact with fibrillin-containing microfibrils within the vessel wall. This interaction not only localises TGF-β to specific sites but also regulates its activation. Mice lacking the long form of LTBP-1 (LTBP-1L)(Todorovic et al., 2007), just like *Tgfb* KO mice (Molin et al., 2004) and neural-crest-specific *Tgfbr2* mutants (Choudhary et al., 2009), die around birth from defects in septation of the heart, cardiac outflow tract, and abnormal remodelling of the pharyngeal arch arteries (PAAs), due to decreased TGF-β signalling (Todorovic et al., 2007).

Interestingly, a recent study has shown that assembly of the glycoprotein fibronectin, rather than fibrillin-1, is essential for incorporation of LTBP-1 into the ECM by vSMCs (Zilberberg et al., 2012). Fibronectin is one of the first ECM proteins to be expressed around the vasculature and is essential for cardiovascular development (Astrof and Hynes, 2009). Fibronectin-null mice die at embryonic day (E)9.5 with defects in the formation of the heart, dorsal aortae and yolk sac vasculature (George et al., 1993; George et al., 1997). Assembly of fibronectin occurs predominantly through the binding of the heterodimeric cell surface adhesion receptor integrin α5β1 to the Arg-Gly-Asp (RGD) motif in fibronectin. In its absence, however, αv integrins (αvβ1, αvβ3, αvβ5, αvβ6, and αvβ8), which also recognise the RGD tripeptide, can relocate to focal contacts previously occupied by α5β1 and assemble fibronectin (Yang and Hynes, 1996; Takahashi et al., 2007; van der Flier et al., 2010). The fibronectin fibrils produced by αv integrins, however, appear short and thick, rather than the long thin dense fibrillar network produced by cells expressing α5β1 (Takahashi et al., 2007; van der Flier et al., 2010).

α5 and αv integrins play key roles in the development of the vasculature (Hynes, 2007). Integrin-α5 KO mice die at E10.5 with severe vascular defects (Yang et al., 1993; Francis et al., 2002; Mittal et al., 2013), while genetic ablation of all five αv integrins leads to placental defects and haemorrhaging within the brain (Bader et al., 1998). Endotheliu̲m-specific deletion of both α5 and αv subunits, however, fails to replicate the angiogenic defects observed in global KO-mice, but instead leads to defects in the remodelling of the heart and great vessels (van der Flier et al., 2010). Interestingly, despite the requirement for both α5 and αv integrins for assembly of fibronectin in vitro, fibronectin fibrils are clearly present within the basement membrane of endotheliu̲m-specific α5/αv mutants (van der Flier et al., 2010), suggesting that fibronectin is assembled by α5 and αv integrins expressed on vSMCs, or by other fibronectin-binding integrins present on the endothelium, such as α4β1 and α9β1.

In vitro, both α5 and αv integrins a̲r̲e̲ essential for regulating the functions of vSMCs (Moiseeva, 2001). Integrin α5β1 is highly expressed on vSMCs and has been shown to promote proliferation, migration, and switching of vSMCs from a more "contractile" to a "synthetic" phenotype (Hedin and Thyberg, 1987; Barillari et al., 2001; Davenpeck et al., 2001; Rensen et al., 2007). Similarly, αv integrins (in particular αvβ3) have been implicated in controlling vSMC migration, de-differentiation, contractility, proliferation and apoptosis (Liaw et al., 1995; D'Angelo et al., 1997; Panda et al., 1997; Dahm and Bowers, 1998). However, the role of α5 and αv integrins on vSMCs in vivo remains unclear. Deletion of α5 using *Pdgfrb-Cre*, which targets both pericytes and vSMCs, results in embryonic lethality due to lymphatic, rather than vSMC defects (Turner et al., 2014), while arteries in the retinas of mice completely deficient in αvβ3 display only minor delays in recruitment and attachment of vSMCs (Scheppke et al., 2012). Therefore, to gain further insight into the functions of both α5 and αv integrins in vivo, we have generated mice that lack *Itga5* and *Itgav* specifically within their vSMCs.

Materials and Methods

Mouse lines

All mouse strains were on 129S4:C57BL/6 mixed background. *Itga5* floxed (van der Flier et al., 2010), *Itgav* floxed (Lacy-Hulbert et al., 2007), mTmG (Muzumdar et al., 2007), Rosa lacZ (Soriano, 1999), *Sm22α-Cre* (Holtwick et al., 2002), and *Wnt1-Cre* (Danielian et al., 1998) mouse lines have all been described previously. Genotyping was performed on DNA isolated from tail snips in-house or by Transnetyx.

Micro-CT scans

4% PFA-fixed embryos were sent to Numira Biosciences (Salt Lake City, UT) for micro-CT imaging. Specimens were stained with a proprietary contrast agent. A high-resolution volumetric micro-CT scanner (μCT40 ScanCo Medical, Zurich, CH) was used to scan the tissue with the following parameters: 6μm isometric voxel resolution at 200ms exposure time, 2000 views and 5 frames per view. The micro-CT generated DICOM files, which were analyzed using OsiriX and Volocity software.

vSMC isolation and culture

vSMCs were isolated from the aortic arch and carotid arteries of *Itga5* flox/flox; *Itgav* flox/flox mice as per Ray et al. (2001) (See Supplemental Materials and Methods). Upon confirmation of vSMC identity by αSMA- and smoothelin-positive immunofluorescence staining, cells were immortalised using SV40 large T antigen (Zhao et al., 2003) and infected with either empty vector or Cre-expressing adenovirus (Gene Transfer Vector Core, University of Iowa, USA) to generate control or Itgα5/αv-deficient vSMCs (ΔItgα5/αv), respectively. Following excision, both control and ΔItgα5/αv cells were grown on plates coated with 20μg/ml Matrigel (BD Bioscience). To generate vSMCs lacking either α5 or αv integrins, ΔItgα5/αv cells were infected with retroviral constructs containing human α5 (van der Flier et al., 2010) or human αv subcloned into LZRS-ms-IRES-zeo construct to generate ΔItgαv or ΔItgα5 cells.

Cell adhesion assays

96-well plates were coated overnight at 4°C with serial dilutions of fibronectin, collagen I, laminin, vitronectin, Matrigel, or recombinant human LAP (TGFβ1) (R&D systems). After blocking with 5% BSA, 20,000 cells/well were plated and allowed to adhere for 24h. Unattached cells were removed by aspiration and adherent cells fixed with 4% PFA and stained with 0.1% Crystal Violet. To quantify adhesion, cells were permeabilised in 50 μl of PBS/0.2% Triton X-100, and OD590 measured in a plate reader.

Cell Shape analysis

Cells were seeded at low density and allowed to adhere to Matrigel-coated glass coverslips for 24h. The cells were then fixed and stained with phalloidin and DAPI. Following imaging of 6 fields from each coverslip, images were automatically analyzed using Volocity software to detect the outline of the cells. Cells touching other cells, or the border of the image, were rejected from the analysis and the shape factor calculated using the formula ($4 \times \pi \times \text{Area} / \text{Perimeter}^2$). A circular cell shape will give a factor of 1 whereas a complex cell

shape will give values close to 0.

DOC insolubility assays

vSMCs were seeded at confluence (200,000 cells/ml) on Matrigel-coated plates in fibronectin-depleted medium in the presence or absence of exogenous biotinylated human fibronectin (10 μg/ml). At 1, 3, and 5 days post-plating, medium was collected, and cells lysed in 0.5 ml DOC buffer [2 mM EDTA, 1% sodium deoxycholate, 20 mM Tris pH 8.5, Complete Mini-protease Inhibitors (Roche)] for fibronectin experiments or 0.25% DOC for investigation of LTBP1 incorporation into the insoluble matrix fraction. After passing eight times through a 22G needle, DOC-insoluble material was spun down for 20 minutes at 20,000 g at 4°C and solubilized in 120 μl 2× reducing SDS-PAGE loading buffer. Reduced (100 mM DTT) samples were loaded onto 4-12% gels.

See Supplemental Material and Methods for details of histology, immunofluorescence staining, immunoblotting, and Real-time RT-PCR.

Results

Sm22α-Cre-mediated deletion of both α5 and αv integrins leads to late embryonic lethality

To investigate the role of α5 and αv integrins on vSMCs in vivo, we crossed female double homozygous *Itga5*/*Itgav*-floxed mice to a male double heterozygous *Itga5*/*Itgav* KO mouse carrying *Sm22α-Cre* recombinase. *Sm22α-Cre* is expressed within differentiated vSMCs throughout the vasculature (Fig. S1) (Holtwick et al., 2002; Yang et al., 2010). This generated four informative genotypes: (1) Control mice, (2) α5 integrin-deficient mutants (hereafter referred to as $Itga5^{Sm22\text{-}Cre}$), (3) αv integrin-deficient mutants (hereafter $Itgav^{Sm22\text{-}Cre}$), and (4) α5/αv conditional double KO mutants (hereafter $Itga5/av^{Sm22\text{-}Cre}$). Examination of offspring revealed that both $Itga5^{Sm22\text{-}Cre}$ *and* $Itgav^{Sm22\text{-}Cre}$ mutants survive embryonic development, but display high rates (~50%) of postnatal lethality (Fig. S2). *Sm22α-Cre*-mediated deletion of both α5 and αv integrins however, resulted in embryonic lethality from E16.5, and no living $Itga5/av^{Sm22\text{-}Cre}$ mice were ever obtained after birth (Fig. S2). Analysis of late gestation mice revealed development of extensive vasculature and no obvious haemorrhaging or oedema in any of the mutant embryos (Fig. S3), however a small number of $Itga5/av^{Sm22\text{-}Cre}$ embryos did appear slightly growth retarded and occasionally pale in colour.

$Itga5/av^{SM22\text{-}Cre}$ mutant mice display abnormal remodelling of the pharyngeal arch arteries (PAAs) and cardiovascular defects

To determine the cause of lethality in $Itga5/av^{Sm22\text{-}Cre}$ mice, mutant embryos were isolated at E17.5 and imaged using a micro-CT scanner. This revealed that $Itga5/av^{Sm22\text{-}Cre}$ embryos develop severe cardiovascular defects (Fig. 1). In contrast to control, $Itga5^{Sm22\text{-}Cre}$ and $Itgav^{Sm22\text{-}Cre}$ embryos, where the aorta arises from the left ventricle and arches over the heart and descends posteriorly as the descending aorta (Fig. 1A), in $Itga5/av^{Sm22\text{-}Cre}$ mice, the ascending aorta misses its connection to the descending aorta (Fig. 1B, C). Since the missing portion of the aortic arch is between the left carotid and subclavian arteries, this is equivalent to the clinically defined type-B interrupted aortic arch. Micro-CT scans also revealed that E17.5 $Itga5/av^{Sm22\text{-}Cre}$ embryos displayed a large aneurysm at the brachiocephalic artery and the proximal region of the right carotid artery (Fig.1B). Interestingly, interrupted aortic arch type-B is also seen in several TGF-β signalling mutants (Molin et al., 2004; Todorovic et al., 2007; Choudhary et al., 2009). Furthermore, neural crest-specific *Tgfbr2* mutants (herein referred to as $Tgfbr2^{Wnt1\text{-}Cre}$) display an interrupted aortic arch and an aneurysm in the brachiocephalic region just as observed in $Itga5/av^{Sm22\text{-}Cre}$ embryos (Choudhary et al., 2009).

In addition to abnormal remodelling of the PAAs, $Itga5/av^{Sm22\text{-}Cre}$ embryos also displayed defects in septation of the outflow tract (conotruncus) and ventricles of the heart (Fig. 1D-G). In wild-type mice, cardiac septation is usually complete between E13.5-E14.5 (Savolainen et al., 2009)(Fig. 1D). However by E17.5, $Itga5/av^{Sm22\text{-}Cre}$ mutants had failed to separate the most proximal region of the outflow tract into the aorta and pulmonary artery (Fig. 1E), a defect known as persistent truncus arteriosus (PTA), and were missing the rostral portion of the ventricular septum (Fig. 1G). Surprisingly, despite these severe defects in development of the heart and aortic arches, no obvious vascular defects were

observed in other tissues analysed. Whole-mount immunofluorescence staining of blood vessels within the skin revealed that α5/αv-deficient mesodermal vSMCs appeared indistinguishable from control cells. vSMCs surrounding dermal arteries in *Itga5/av*$^{Sm22\text{-}Cre}$ embryos appeared aligned, tightly attached and expressed high levels of the contractile protein α-smooth muscle actin (αSMA) (Fig. 1H).

Neural crest-specific ablation of both α5 and αv integrins leads to cardiovascular defects

During early embryonic development (at ~E9.5 in mice), cardiac neural crest cells (CNCCs) from the dorsal neural tube migrate along the 3rd, 4th and 6th pharyngeal arch arteries (PAAs) and invade the cardiac outflow tract of the heart, where they proliferate, condense and form the aorticopulmonary septum which divides the single-tubed vessel into the ascending aorta and pulmonary trunk (Kirby et al., 1983; Kirby and Waldo, 1995; Jiang et al., 2000). In addition, CNCCs covering the PAAs have a separate role and differentiate into vSMCs and help co-ordinate patterning of the aortic arch arteries. The physiological importance of CNCCs in development of the cardiovascular system can be seen in ablation studies carried out in chicken embryos. Loss of CNCCs leads to abnormal remodelling of the aortic arches, defects in the septation of the outflow tract, and disrupted formation of the thymus (Kirby and Waldo, 1995).

Since vascular defects were observed in *Itga5/av*$^{Sm22\text{-}Cre}$ embryos only in areas known to be dependent on CNCCs, we crossed female double homozygous *Itga5/Itgav*-floxed mice (*Itga5*$^{flox/flox}$; *Itgav*$^{flox/flox}$) to male double heterozygous *Itga5/Itgav* KO mice carrying the *Wnt1-Cre* recombinase (*Itga5*$^{+/-}$; *Itgav*$^{+/-}$; *Wnt1-Cre*$^{+}$), to test whether the phenotype of *Itga5/av*$^{Sm22\text{-}Cre}$ embryos was in fact due to defects in neural crest-derived cells. As expected, *Wnt1-Cre* was expressed throughout the neural crest (Fig. S4A), and in vSMCs surrounding the ascending aorta, aortic arch and carotid arteries (Fig. 2A).

Consistent with an essential role for α5 and αv integrins in neural crest function (Mittal et al., 2010), most *Itga5*$^{Wnt1\text{-}Cre}$, *Itgav*$^{Wnt1\text{-}Cre}$, and *Itga5/av*$^{Wnt1\text{-}Cre}$ mutants died at around birth (Fig. S5). However, only *Itga5/av*$^{Wnt1\text{-}Cre}$ mutants displayed cardiovascular defects (Fig. 2B-G). Just as observed in *Itga5/av*$^{Sm22\text{-}Cre}$ mutants, *Itga5/av*$^{Wnt1\text{-}Cre}$ embryos developed PTA (Fig2B-E), and ventricular septal defects (Fig. 2F and G), confirming that the phenotype of *Itga5/av*$^{Sm22\text{-}Cre}$ is largely due to loss of α5 and αv integrins on CNCCs. Genetic deletion of both α5 and αv integrins did not appear to affect neural crest cell distribution in early *Itga5/av*$^{Wnt1\text{-}Cre}$ mutants however. Analysis of whole-mount Xgal-stained *Itga5/av*$^{Wnt1\text{-}Cre}$ embryos containing the Rosa26LacZ reporter revealed an overtly normal pattern of neural crest cells in mutant mice (Fig. S4A-D). Moreover, CNCCs were clearly present in the outflow tracts of E11.5 *Itga5/Itgav*$^{Wnt1\text{-}Cre}$ mutants (Fig. S4B and D), indicating that loss of both α5 and αv integrins does not compromise CNCC migration. However, in contrast to *Itga5/av*$^{Sm22\text{-}Cre}$ embryos, *Itga5/av*$^{Wnt1\text{-}Cre}$ embryos rarely developed defects in remodelling of the aortic arch (1/6) and never developed the large aneurysms at the brachiocephalic artery (Fig. 2C) suggesting that the remodelling of the PAAs may be dependent on both mesodermal and neural-crest-derived vSMCs.

***Itga5/Itgav*$^{Wnt1\text{-}Cre}$ mice have ectopically located thymi and cleft palate**

In addition to cardiovascular defects, *Itga5/av*$^{Wnt1\text{-}Cre}$ mice also displayed defects in the positioning of their thymus. At E17.5, the two lobes of the thymus should be positioned above the heart (Fig. 2H). In *Itga5/av*$^{Wnt1\text{-}Cre}$ embryos however, at least one lobe of the thymus was often ectopically located in the cervical region (Fig. 2I). Once again, mirroring the defects in *Tgfbr2*$^{Wnt1\text{-}Cre}$ mutants (Ito et al., 2003), *Itga5/Itgav*$^{Wnt1\text{-}Cre}$ mice also developed a cleft palate (Fig. 2J, K). Fusion of palatal shelves is normally complete by E14.5 in control mice. Palatal shelves in *Itga5/Itgav*$^{Wnt1\text{-}Cre}$ mice however, remained small and failed to fuse at the midline by E17.5 (Fig. 2K).

Normal vSMC differentiation in *Itga5/av*$^{SM22\text{-}Cre}$ mutants

A critical step in the formation of the great arteries is the differentiation of CNCCs into highly contractile vSMCs. Neural-crest-specific deletion of *Tgfbr2* (Wurdak et al., 2005), *Smad2* (Xie et al., 2013), *Notch* (High et al., 2007) or the myocardin-related transcription factor B (Li et al., 2005), all lead to defects in vSMC differentiation and abnormal development of the outflow tract and aortic arch arteries. Failure to differentiate CNCCs into vSMCs was not the cause of the defects in *Itga5/av*$^{SM22\text{-}Cre}$ embryos however**.** Expression of the early vSMC markers αSMA and smooth muscle myosin heavy chain 11 (Myh11) were clearly visible in CNCC-derived cells surrounding the brachiocephalic artery (Fig. S6A) and PAA (data not shown) at E11.5 and continued to be expressed around the great vessels until lethality at E17.5 (Fig. S6B-D).

Abnormal vSMC morphology in the right carotid artery of *Itga5/av*$^{SM22\text{-}Cre}$ mutants

Although the differentiation of vSMCs appeared unaffected by the loss of α5 and αv integrins, immunofluorescence staining of E17.5 embryos with anti-αSMA antibodies did reveal striking abnormalities in the structure of the ascending aorta, carotid and brachial arteries in *Itga5/av*$^{SM22\text{-}Cre}$ mice. In control embryos, vSMCs appeared long, compact, and were organised into 3-4 concentric lamellar units within the vessel wall (Fig. 3A, C). In contrast, vSMCs in the ascending aorta (data not shown) and right carotid/brachiocephalic artery of mutant embryos appeared round, disorganised and formed up to 18 layers of cells (Fig. 3B, D). Furthermore, in the most severely affected mutants, PECAM-1-positive endothelial cells were undetectable within the aneurysm (Fig. 3B). Large regions of the great vessels appeared unaffected by the loss of both α5 and αv integrins however. vSMCs around the left carotid artery of *Itga5/av*$^{SM22\text{-}Cre}$ embryos for example appeared well organised despite often displaying an increased number of lamellar units (Fig. S6B). In addition, no obvious defects in vSMC proliferation could be detected around the brachiocephalic or carotid arteries (Fig. S7).

ECM deposition within the right brachiocephalic/carotid artery is disrupted in *Itga5/av*$^{SM22\text{-}Cre}$ mutants

Previous studies have shown that the assembly of ECM proteins within the vessel wall is essential for maintaining the structural integrity of the great vessels. We therefore examined whether the dilated brachiocephalic/carotid artery in *Itga5/av*$^{SM22\text{-}Cre}$ embryos was due to abnormal ECM deposition.

Surprisingly, despite the requirement for both α5 and αv integrins for fibronectin fibrillogenesis in vitro, fibronectin fibrils were clearly visible in the vessel walls of both

early (Fig. S8) and late (Fig. 4A) gestation *Itga5/av*$^{SM22\text{-}Cre}$ embryos. In contrast to control mice these fibrils displayed a disorganised lamellar organisation at E17.5 (Fig. 4A). The assembly of microfibril ECM proteins was also disrupted in *Itga5/av*$^{SM22\text{-}Cre}$ embryos. In the dilated carotid arteries of mutant mice, fibrillin-1-containing microfibrils were almost undetectable in the tunica media, and organisation of fibulin-5 into lamellar structures appeared impaired (Fig. 4B and C). As observed in most human aneurysms, *Itga5/av*$^{SM22\text{-}Cre}$ embryos also displayed elastin fragmentation within their aneurysm (Fig. 4D). Furthermore, collagen IV fibrils, which are also found in the medial layers, were largely absent from the aneurysmal region of mutant mice (Fig. 4E). Thus, the disorganised pattern of vSMCs is accompanied by defects in organisation of several ECM proteins.

Loss of integrin α5 and αv disrupts focal adhesion formation and signalling via Paxillin and FAK.

To gain further insight into the molecular mechanisms underlying the *Itga5/av*$^{SM22\text{-}Cre}$ phenotype, vSMCs from the aortae of adult *Itga5/av*$^{flox/flox}$ mice were isolated and immortalised with the SV40 large T antigen. vSMC identity was confirmed by immunofluorescence staining for αSMA and smoothelin (Fig. 5A). Integrin α5/αv floxed cells were then infected with either an empty vector or Cre-expressing adenovirus to generate control and integrin α5/αv-deficient vSMCs (ΔItgα5/αv) respectively. Efficient excision of the floxed alleles was confirmed by PCR (data not shown) and loss of both α5 and αv proteins verified by immunoblotting (Fig. 5B). Consistent with the binding affinities of α5 and αv, ΔItgα5/αv cells failed to attach to either fibronectin or vitronectin (Fig. 5C), and showed reduced adhesion to both laminin and collagen I substrates (Fig. S9A), despite expressing similar levels of their cognate integrin receptors (Fig. S9B). ΔItgα5/αv cells however, adhered efficiently to Matrigel (Fig. 5C), but appeared smaller and more rounded, and had fewer protrusions than control cells 24h after plating (Fig. 6A-C).
Visualisation of the contacts between the cells and the ECM revealed that loss of both α5 and αv had dramatic effects on the formation of mature adhesions. In control vSMCs, focal adhesions are visible in cell protrusions and are present as fibrillar adhesions in the cell body (Fig. 6A and D). In contrast, ΔItgα5/αv cells contain only nascent adhesions and focal complexes throughout the cell (Fig. 6B and E). As a result, ΔItgα5/αv cells show reduced activation of the focal adhesion kinase (FAK), markedly reduced levels of paxillin phosphorylation, and reduced phosphorylation of the Crk-associated substrate p130(CAS) (Fig. 6F, quantifications in Fig. S9C). These deficits were rescued by re-expression of either *Itga5* or *Itgav* within ΔItgα5/αv cells (Fig. 6F) suggesting that either integrin can compensate for loss of the other.

Loss of α5 and αv integrins leads to abnormal TGF-β signalling

Given the similarity of the cardiovascular defects observed in *Itga5/av*$^{SM22\text{-}Cre}$ mutants and knockouts of *LTBP-1L* (Todorovic et al., 2007) or *TGFβ* (Molin et al., 2004), and mice in which the *Tgfbr2* gene was conditionally ablated in vSMC precursors (Choudhary et al., 2009), we examined whether TGF-β signalling was disrupted in our ΔItgα5/αv cells. Immunoblotting for downstream mediators of the canonical TGF-β signalling pathway revealed that phosphorylation of SMAD2, but not SMADs 1, 5, and 8 (Fig. 7A), was reduced in ΔItgα5/αv cells, despite a moderate increase in *Tgfb1* expression (Fig. S9D). The extent

of this reduction in SMAD signalling appeared dependent on the Matrigel batch used, with some experiments producing only small changes in the level of pSMAD2 on specific Matrigel preparations (data not shown). To our surprise, immunofluorescence staining revealed that pSMAD2 levels were increased in the aneurysmal region of *Itgα5/αv*$^{SM22\text{-}Cre}$ embryos, when compared to the right carotid artery of control E17.5 mice (Fig. 7B). Interestingly, this increase was also apparent, just before the onset of the large dramatic aneurysm, in the brachiocephalic/carotid region in E12.5 embryos (Fig. S10). However, no obvious differences in pSMAD2 signalling were observed in any of the other regions of *Itgα5/αv*$^{SM22\text{-}Cre}$ embryos examined (Fig. 7B).

α5β1 and αv integrins bind to the Latency-associated protein (LAP)

TGF-β is secreted as an inactive form and requires release from LAP to exert its biological functions. Previous studies have shown that integrins regulate TGF-β signalling by interacting with the RGD motif contained in the LAPs of TGF-β1 and TGF-β3 releasing TGF-β from its latent complex (Munger et al., 1999; Annes et al., 2002; Yang et al., 2007). To determine whether loss of both α5 and αv prevented binding to LAP, we assessed the ability of control, ΔItgαv, ΔItgα5 and ΔItgα5/αv vSMCs to adhere to recombinant human TGF-β1 LAP-coated plates. Consistent with previous data (Munger et al., 1998; Munger et al., 1999; Ludbrook et al., 2003), loss of integrin αv significantly reduced binding to LAP (Fig. 7C). Adhesion to LAP was also reduced in ΔItgα5 vSMCs, albeit to lesser extent than in ΔItgαv cells, while binding to LAP was almost completely blocked in cells lacking both α5 and αv integrins (Fig. 7C).

Integrin α5 and αv are required for incorporation of LTBP-1 but not LTBP-3 into the ECM

Integrin binding to LAP alone is not sufficient for TGF-β activation. The complex of TGF-β and LAP (small latent complex) also requires anchoring to the ECM through its association with LTBP1 and LTBP3 (Horiguchi et al., 2012). For LTBP1, this incorporation is dependent on the assembly of fibronectin, and is independent of fibrillin expression, whereas incorporation of LTBP3 is dependent on assembly of fibrillin-1 microfibrils (Zilberberg et al., 2012). To examine whether ΔItgα5/αv vSMCs could incorporate LTBP1 into the matrix, we first analysed the ability of ΔItgα5/αv vSMCs to assemble endogenous fibronectin into fibrils. Immunofluorescence staining revealed that control vSMCs form extensive fibronectin fibrils 24 hours after plating (Fig. 7D). In contrast, ΔItgα5/αv vSMCs plated at confluency, formed smaller aggregates of fibronectin (Fig. 7D). Since fibronectin mRNA expression levels were reduced (30-40%) in cells lacking both α5 and αv (Fig. S11A), we analysed the ability of ΔItgα5/αv vSMCs to incorporate exogenous biotin-labelled fibronectin into the DOC-insoluble matrix (Fig. S11B). This revealed that, even after 5 days in culture, ΔItgα5/αv vSMCs are unable to assemble exogenous fibronectin into fibrils (Fig. S11B). Re-expression of either α5 or αv integrin however, rescued the ability of ΔItgα5/αv vSMCs to assemble and incorporate fibronectin into the DOC-insoluble matrix (Fig. 7E). Similarly, ΔItgα5/αv vSMCs also had defects in their ability to assemble the RGD-containing microfibrillar proteins, fibrillin-1 and fibulin-5 in vitro (Fig. 7E). Surprisingly, in contrast to our in vivo results, lack of fibrillin-1 and fibulin-5 did not affect

the deposition of elastin (Fig. 7E). Loss of α5 and αv integrins did affect incorporation of the RGD-containing LTBP1 into the DOC-insoluble matrix however (Fig. 7F). After 3 days in culture, LTBP1 was incorporated into the ECM by control, and to lesser extent ΔItgα5 and ΔItgαv vSMCs, but was completely absent from the ECM assembled by ΔItgα5/αv cells (Fig. 7F). Interestingly, incorporation of LTBP3, which does not contain an RGD motif, appeared unaffected by loss of α5 and αv and the lack of fibronectin and fibrillin-1 fibrils (Fig. 7F). Thus, absence of these two integrin subunits on vSMCs compromises assembly of ECM proteins and components of TGFβ signalling complexes.

Discussion

In this study, we have shown that α5 and αv integrins on neural crest-derived vSMCs cooperate to control remodelling of the PAAs and are essential for the septation of the heart and outflow tract. We have also shown that vSMC expression of both α5 and αv subunits are essential for assembly of ECM within the vessel wall and that loss of both integrins leads to the formation of large aneurysms within the brachiocephalic/carotid arteries. Expression of α5 and αv integrins however appears to be dispensable for initial assembly of an extensive vascular network and the function of vSMCs surrounding vessels in the skin.

Cardiovascular development is regulated by α5 and αv integrins

Consistent with our previous study (Turner et al., 2014), genetic ablation of α5β1 from vSMCs failed to replicate any of the vascular defects observed in the global *Itga5* KO mice (Yang et al., 1993; Francis et al., 2002). *Itga5*$^{SM22\text{-}Cre}$ mice survived to birth with no obvious vSMC or cardiovascular defects. Similarly, despite numerous studies suggesting that αv integrins play a key role in controlling vSMC function in vitro (Liaw et al., 1995; D'Angelo et al., 1997; Panda et al., 1997; Dahm and Bowers, 1998), *Itgav*$^{SM22\text{-}Cre}$ mutants developed normally and contained blood vessels indistinguishable from those in control mice. Both *Itga5*$^{SM22\text{-}Cre}$ and *Itgav*$^{SM22\text{-}Cre}$ mice displayed postnatal lethality however, suggesting that loss of either integrin may increase susceptibility to cardiovascular defects after birth. Although contradictory to numerous blocking studies in vitro, the lack of major vascular defects in *Itga5*$^{SM22\text{-}Cre}$ and *Itgav*$^{SM22\text{-}Cre}$ embryos fits with a growing body of data showing that α5 and αv integrins have overlapping functions and that either integrin can compensate for loss of the other (Yang and Hynes, 1996; Takahashi et al., 2007; van der Flier et al., 2010). Indeed, ablation of *Itga5* or *Itgav* alone, caused only a minor reduction in focal adhesion signalling and matrix assembly in our cultured vSMCs. It is also possible that some integrin functions, such as assembly of ECM matrix or activation of TGF-β, are compensated for by integrins expressed on adjacent cells within the vasculature. This may help explain why tissue-specific integrin mutants often display phenotypes less severe than those predicted from in vitro studies.

In contrast with the results for single *Itga5*$^{SM22\text{-}Cre}$ and *Itgav*$^{SM22\text{-}Cre}$ mutants, deletion of both α5 and αv integrins by *SM22α-Cre* caused significant cardiovascular defects. *Itga5/av*$^{SM22\text{-}Cre}$ embryos developed interrupted aortic arch type-B and a large aneurysm that encompassed the brachiocephalic artery and the proximal region of the right carotid artery. The same phenotype has been observed in mice that lack vSMC expression of all the β1 integrins (Turlo et al., 2012). This suggests that the phenotype of *Itga5/av*$^{SM22\text{-}Cre}$ mice, and therefore the vSMC-specific *Itgb1* mutant, is caused by the loss of α5β1 and specifically αvβ1, rather than any of the other αv (αvβ3, αvβ5, αvβ6, and αvβ8) or β1 (α1β1, α2β1, α3β1, α4β1, α6β1, α7β1, α9β1, α10β1, α11β1) integrin heterodimers. Like Turlo et al. (2012) we also found that migration and initiation of vSMC fate were unaffected by loss of α5 and αv integrins. vSMC in *Itga5/av* mutants expressed high levels of vSMC markers αSMA, SM22α, and Myh11, and migrated efficiently to the PAAs and blood vessels within the skin. Deletion of both α5 and αv integrins also appeared to have no obvious effect on

the functions of mesodermally derived vSMCs during embryonic development. In contrast to mural cell-specific *Itgb1* mutant mice (Abraham et al., 2008), in which vSMCs appeared round, poorly spread and only loosely attached to the subendothelial basement membrane, vSMCs in the cutaneous vasculature of *Itga5/av*$^{SM22\text{-}Cre}$ embryos appeared indistinguishable from those in control mice. One possible explanation for these conflicting results is that vascular defects in mural-cell-specific *β1* mutants are due to loss of *Itgb1* on pericytes, rather than vSMCs. Alternatively, β1 heterodimers, other than α5β1 and αvβ1, may play important roles in mesodermally derived vSMCs; defects in pericyte and vSMC distribution have been reported in α4 and α7-KO mice (Flintoff-Dye et al., 2005; Garmy-Susini et al., 2005; Grazioli et al., 2006). Arguing against this latter hypothesis, however, is the fact that vascular defects also appear to be restricted to areas populated by neural-crest-derived vSMCs in mice in which *Itgb1* has been deleted in all vSMCs, using the same *SM22α-Cre* line used in this study (Turlo et al., 2012). Nevertheless, large aneurysms are found both in *β1* mutants (Abraham et al., 2008; Turlo et al., 2012) and in our *Itga5/av*$^{SM22\text{-}Cre}$ embryos. As in the vSMC-specific *β1* mutants (Turlo et al., 2012), aneurysms were present only in the brachiocephalic and carotid arteries. This could be due to these regions' exhibiting the greatest shear stress (Meng et al., 2007; Huo et al., 2008; Wang et al., 2009), especially when flow is re-directed to the brachiocephalic and right carotid artery when the aortic arch is interrupted. These regions of the vasculature also correlate with areas where expression of integrin β1 is highest (Turlo et al., 2012). It is possible therefore that the aorta, brachiocephalic and carotid artery are more sensitive to the loss of *Itga5* and *Itgav*, and may suggest that both α5β1 and αvβ1 integrins play an important role in providing structural strength to the blood vessels and resisting the high pulsatile flow from the heart. Alternatively, these regions may be more susceptible due to being populated by different subsets of CNCCs, compared to other parts of the great vessels, and heightened expression of β1 integrins may simply correlate with a specific population of vSMCs. Interestingly, decreased expression of *ITGA5* has previously been linked to formation of human aortic aneurysms (Cheuk and Cheng, 2004) and, similar to some human aneurysms (Pera et al., 2010) and experimentally induced aneurysms in mice (Murphy and Hynes, 2014), PECAM-1-positive endothelial cells were reduced in the dilated brachiocephalic artery of *Itga5/av*$^{SM22\text{-}Cre}$ mice at late stages. It is unclear however, whether this loss is specifically linked to deletion of both α5 and αv within vSMCs, or merely part of the general pathology occurring within a large aneurysm. It is conceivable that defects in vSMC function (assembly of the basement membrane ECM, signalling, contraction) may be directly, or indeed indirectly, causing this dedifferentiation. After all, mechanosensing by PECAM-1 is directly linked to integrin engagement to the ECM (Collins et al., 2012), PECAM-1 is a ligand for αvβ3 (Piali et al., 1995) and is regulated by TGF-β (Neubauer et al., 2008).

Since *SM22α-Cre* is also expressed in the heart (Turlo et al., 2012), we cannot definitively rule out the possibility that the *Itga5/av*$^{SM22\text{-}Cre}$ phenotype is secondary to heart defects. Development of the aortic arch has been shown to be linked to the haemodynamics of blood flowing from the heart (Yashiro et al., 2007). However, as septation and PTA defects were also found in *Itga5/av*$^{Wnt1\text{-}Cre}$ embryos, which lacked aneurysms and aortic arch defects, and because *Itga5/av*$^{SM22\text{-}Cre}$ mice developed dilated brachiocephalic/carotid arteries before cardiac septation at E12.5, we think this is unlikely. We believe instead,

since both neural crest and mesenchyme-derived cells contribute to the aorta and PAAs (Bergwerff et al., 1998), that the vascular defects are less severe in *Itga5/av*$^{Wnt1\text{-}Cre}$ embryos, since α5/αv-containing mesenchyme-derived cells can compensate, at least in part, for the loss of both integrins in the neural-crest-derived vSMCs.

α5 and αv integrins are essential for neural crest functions in vivo

In our attempts to further understand the cardiovascular defects in our mutants, we have also investigated the ways in which α5 and αv integrins cooperate to regulate neural crest function. Almost all *Itga5*$^{Wnt1\text{-}Cre}$ embryos died shortly after birth, while *Itgav*$^{Wnt1\text{-}Cre}$ and, to a greater extent, *Itga5/av*$^{Wnt1\text{-}Cre}$ mutants displayed perinatal lethality. The loss of *Itga5/av*$^{Wnt1\text{-}Cre}$ mice is considerably later than the lethality seen in neural crest-specific *Itgb1* mutants (Turlo et al., 2012), confirming the importance of other β1-containing receptors in neural crest cells. Both cardiac and cranial neural crest defects were observed in *Itga5/av*$^{Wnt1\text{-}Cre}$ mutants. In addition to developing a PTA and VSDs, *Itga5/av*$^{Wnt1\text{-}Cre}$ mice also displayed mislocated thymi and cleft palate. Previous studies have shown that migration of neural crest cells is dependent on α5 and αv expression and defects in neural crest migration can lead to heart, thymus and craniofacial defects (Delannet et al., 1994; Alfandari et al., 2003; Keyte and Hutson, 2012). Migration defects do not appear to be the cause, at least of the cardiovascular defects, in *Itga5/Itgav*$^{Wnt1\text{-}Cre}$ mutants. Although we cannot rule out relatively subtle defects in the migration of specific subsets of neural crest cells, *Wnt1*-positive CNCCs were clearly present in the PAA and outflow tracts in *Itga5/Itgav*$^{Wnt1\text{-}Cre}$ embryos as early as E11.5. These results are consistent with a number of studies showing that septation and PAA defects can occur independently from neural crest migration and differentiation defects (Molin et al., 2004; Turlo et al., 2012).

Role of α5 and αv integrins in cardiovascular development

So how do α5 and αv integrins regulate cardiovascular development? Our analysis of ΔItgα5/αv vSMCs in vitro suggests a number of possibilities. First, our data show that loss of the α5 and αv integrins prevents the formation of mature focal adhesions and, as a consequence, leads to reduced levels of FAK and paxillin phosphorylation. Focal adhesions are essential for maintaining structural integrity of vessels by inducing cytoskeletal rearrangements and alignment of vSMCs in response to mechanical strain. Previous studies have shown that genetic deletion of FAK (*Ptk2*) in vSMC precursors leads to defects in the patterning of the aortic arch arteries and septation of the heart and outflow tract (Hakim et al., 2007; Vallejo-Illarramendi et al., 2009; Cheng et al., 2011). These defects however are caused by abnormal recruitment (Hakim et al., 2007; Cheng et al., 2011), and/or impaired differentiation of vSMCs (Vallejo-Illarramendi et al., 2009), neither of which is seen in our mutants. Less information exists about the role of paxillin in vSMCs. In vitro, paxillin has been implicated in regulating adhesion, proliferation, apoptosis and activation of L-type calcium channels in vSMCs (Wu et al., 2001; Veith et al., 2012). To date, no one has investigated the role of paxillin specifically in vSMCs in vivo. Intriguingly however, paxillin KO mice die at E9.5 with cardiac and somatic defects resembling those in fibronectin KO mice (Hagel et al., 2002).

The cardiovascular defects in *Itga5/av*$^{SM22\text{-}Cre}$ mice may also be due to the inability of

ΔItgα5/αv vSMCs to interact correctly with the ECM. ΔItgα5/αv vSMCs failed to attach to either fibronectin or vitronectin, and displayed reduced adhesion to laminin and collagen I. As a result, ΔItgα5/αv vSMCs often appeared poorly spread in vitro and mirrored the round disorganised morphology of vSMCs within the ascending aorta, brachiocephalic and right carotid artery of *Itga5/av*$^{SM22\text{-}Cre}$ embryos. Our data also indicate that α5 and αv integrins are required for the assembly and organisation of the ECM within the vessel wall. In vitro, consistent with α5 and αv being the predominant RGD-binding receptors expressed on vSMCs, ΔItgα5/αv vSMCs were unable to incorporate fibronectin, fibrillin-1, or fibulin-5 into the DOC-insoluble ECM. Furthermore, organisation of the ECM into concentric lamellar layers around the ascending aorta, brachiocephalic and carotid artery appeared severely compromised in *Itga5/av*$^{SM22\text{-}Cre}$ mice. Correct assembly of the ECM is essential for maintaining vascular integrity; vSMCs alone are insufficient to resist the mechanical strain generated by pulsatile blood flow (Wagenseil and Mecham, 2009). Defects in assembly of fibrillin, fibulin, collagen and elastin have all been implicated in the formation of aneurysms in vivo (El-Hamamsy and Yacoub, 2009). It is likely therefore, that the abnormal assembly of the ECM weakens the vessel wall and directly causes the aneurysms in *Itga5/av*$^{SM22\text{-}Cre}$ embryos.

A final intriguing possibility is that the defects in *Itga5/av*$^{SM22\text{-}Cre}$ mice are in fact related to abnormal TGF-β signalling. Previous studies have shown that TGF-β signalling is essential for the patterning of the aortic arch, septation of the heart and outflow tract, and for fusion of the palatal shelves and development of the thymus (Ito et al., 2003; Molin et al., 2004; Wang et al., 2006; Todorovic et al., 2007; Choudhary et al., 2009), defects all present in our *Itga5/Itgav* mutants. Furthermore, ΔItgα5/αv vSMCs were unable to bind to LAP, or to deposit LTBP-1 into the ECM and had decreased levels of pSMAD2. Paradoxically, in vivo, *Itga5/av*$^{SM22\text{-}Cre}$ mice displayed increased levels of pSMAD2 within their aneurysms. This "TGF-β paradox" has also been seen in aortic aneurysms present in patients with Loeys-Dietz and Marfan's syndrome, which, in theory, should also exhibit reduced pSMAD2 levels within their vasculature (Lin and Yang, 2010). The exact mechanism for this paradox remains unclear. However, it may be due to excessive (compensatory) upregulation of TGF-β, increased metalloproteinase expression, dysregulation of TGF-β signalling feedback loops, or even through non-TGF-β activators of SMADs (Lin and Yang, 2010). There is also the possibility that the defects in *Itga5/av*$^{SM22\text{-}Cre}$ mice are actually due to reduced non-SMAD TGF-β signalling (Moustakas and Heldin, 2005). Since there is extensive cross talk between TGF-β signalling pathways, integrins, focal adhesions, and the ECM, it is extremely difficult to unravel the exact chain of causality leading to the defects seen in *Itga5/av*$^{SM22\text{-}Cre}$ mice or those in TGF-β signalling.

Role of α5 and αv integrins in initial development of blood vessels

Deletion of both α5 and αv integrins from either vSMCs or endothelial cells (using *Tie2-Cre*) results in defects in the remodelling of the great vessels and the heart, but, in both cases, fails to disrupt initial blood vessel development (van der Flier et al., 2010; Turner et al., 2014), or replicate the phenotypes of the global KO mice (see Introduction). These observations suggest that integrins on both mural cells (pericytes, vSMCs) and endothelial cells cooperate to regulate the assembly of ECM proteins and signalling complexes such as

those for TGF-β within the ECM. It is, of course, possible that some other cell types expressing these integrins play some essential role, although this seems to us less likely.

Conclusion

Congenital heart defects (CHD) are a leading cause of miscarriage and the most common type of birth defect (Bruneau, 2008). Furthermore, as surgical intervention has advanced, and more children with CHD survive into adulthood, there is an even greater need to understand the molecular pathways that regulate cardiovascular development. Our study has shown that α5 and αv integrins are essential for development of the heart and great vessels. However, many questions about their precise roles in vascular development and homeostasis remain unresolved. Future experiments will need to examine the role of α5 and αv integrins in the adult vasculature, and assess whether loss of either integrin subunit, increases susceptibility to aortic aneurysms and other vascular diseases.

Acknowledgements

We thank members of the Hynes laboratory, especially Patrick Murphy, for discussions and advice. This work was supported by grants from the National Institutes of Health (PO1-HL66105, PI, Monty Krieger), the NIGMS Cell Migration Consortium, (GC11451.126452, PI, A.F. Horwitz), by the Koch Institute Support (core) Grant P30-CA14051 from the National Cancer Institute and the Howard Hughes Medical Institute. CJT was a postdoctoral associate and ROH is an Investigator of the Howard Hughes Medical Institute.

Author Contributions

Experiments were conceived, designed and interpreted by CJT, KB-N, AF and ROH. Experiments were performed by CJT, KB-N, and AF; DC provided sections. The manuscript was written by CJT and ROH.

Figure legends

Figure 1. Cardiovascular defects in *Itga5/av*$^{SM22\text{-}Cre}$ mice.
3D-rendered micro-CT images of the pharyngeal arch arteries in E17.5 embryos; (A) control and (B) *Itga5/av*$^{SM22\text{-}Cre}$ mutant embryos displaying an interrupted aortic arch (type-B) with dilation of the brachiocephalic artery and proximal portion of the carotid artery (indicated with an asterisk). The atria have been removed to allow better visualization of the aortic arch. Note that the region of the aortic arch that is derived from the IV pharyngeal arch in the control (Δ, outlined in blue in A, which corresponds with the blue region in C), is missing in the *Itga5/av*$^{SM22\text{-}Cre}$ mutant. (B). (C) Schematic overview of the PAAs (III-red, IV–blue, VI-green) in an E17.5 control and *Itga5/av*$^{SM22\text{-}Cre}$ mutant (modified from (Papangeli and Scambler, 2013). (D and E) Micro-CT sections showing normal septation of the outflow tract into ascending aorta (AoA) and pulmonary trunk (PT) in a control embryo (D) and PTA in an *Itga5/av*$^{SM22\text{-}Cre}$ embryo (E) at E17.5. (F and G) H&E stainings of E17.5 heart sections demonstrating normal cardiac septation in control (F) and ventricular septation defects (VSD) in *Itga5/av*$^{SM22\text{-}Cre}$ embryos (G). (H) Whole-mount immunofluorescence images showing normal association of vSMCs (αSMA, red) around blood vessels (PECAM-1, green) within the skin of (I) control (II) *Itga5*$^{SM22\text{-}Cre}$, (III) *Itgav*$^{SM22\text{-}Cre}$ (IV) and *Itga5/av*$^{SM22\text{-}Cre}$ mutant embryos at E17.5. Abbreviations: RSA/LSA-right/left subclavian artery, RCA/LCA-right/left carotid arteries, BCA-brachiocephalic artery, DA-ductus arteriosus, AoA-ascending aorta, AoD-descending aorta, PAA-pharyngeal arch arteries, PTA persistent truncus arteriousus. Scale bars: 1 mm (D, E), 25 μm (H).

Figure 2. Integrins α5 and αv are essential for cardiac neural crest function.
(A) LacZ staining confirming *Wnt1-Cre* expression in neural crest-derived vSMCs surrounding the aortic arch and carotid arteries of an adult mouse. Vascular casts (blue) showing the patterning of the aortic arch arteries in a control (B) and an *Itga5/av*$^{Wnt1\text{-}Cre}$ embryo with persistent truncus arteriosus (PTA) at E17.5 (C).
(D-K) Micro-CT sections through a control and *Itga5/av*$^{Wnt1\text{-}Cre}$ embryo at E17.5. Instead of displaying a distinct ascending aorta (AoA) and pulmonary trunk (PT) (see D), the outflow tract of *Itga5/av*$^{Wnt1\text{-}Cre}$ embryos remained a single vessel leading to PTA (see E). Complete ventricular septation in a control (F) and VSD in an *Itga5/av*$^{Wnt1\text{-}Cre}$ embryo (G). Correct position of the thymus in a control (H) and ectopic location of both thymic lobes in an *Itga5/av*$^{Wnt1\text{-}Cre}$ embryo (I). Normal formation of the palatal shelf (PS) in control (J) and cleft palate in an *Itga5/av*$^{Wnt1\text{-}Cre}$ embryo (K). Note; inserts in H-K show additional frontal views of scans. Scale bars: 2 mm (B, C), 1 mm (D-I), 2 mm (J, K).

Figure 3. Abnormal vSMC organisation in the brachiocephalic/carotid artery region of *Itga5/av*$^{SM22\text{-}cre}$ embryos.
Transverse sections showing the structure of the right carotid artery in (A) control and (B) *Itga5/av*$^{SM22\text{-}cre}$ embryos at E17.5. Inset in (B) shows the entire right carotid artery in section at lower magnification. Higher magnification images of boxed regions in A and B (C and D). Note the abnormal thickening of arterial wall and disorganised and round morphology of vSMCs in the *Itga5/av*$^{SM22\text{-}cre}$ mutant. Scale bars: 50 μm (A, B).

Figure 4. Deposition of ECM proteins within the vessel wall of *Itga5/av*$^{SM22\text{-}cre}$ embryos.
Immunofluorescence staining of transverse sections through the brachiocephalic/carotid artery of control and the corresponding dilated vessel of *Itga5/av*$^{SM22\text{-}cre}$ embryos at E17.5 showing the deposition of (A) fibronectin, (B) fibrillin-1, (C) fibulin-5, (D) elastin (enlarged in insets) and (E) collagen IV; within the vessel wall. Note the concentric lamellar layers of ECM around the carotid artery in the control mouse (top), and the disorganised ECM within the tunica media in the mutant (bottom). The strong signals in the lumens in some panels arise from non-specific staining of blood cells. Scale bars: 50 μm (A-E).

Figure 5. Generation and characterisation of integrin α5/αv-deficient vSMCs.
(A) Identity of vSMCs was confirmed by staining for αSMA (red) and smoothelin (green). (B) Western blot confirming efficient deletion of α5 and αv integrin subunits following Cre excision in ΔItgα5/αv vSMCs. (C) Cell adhesion assay demonstrating the ability of ΔItgα5/αv vSMCs to adhere to Matrigel, but not to fibronectin or vitronectin substrates. Scale bar: 10 μm (A).

Figure 6. Abnormal focal adhesion formation in ΔItgα5/αv vSMCs.
(A-B) Double immunofluorescence stainings showing the actin cytoskeleton (red) and distribution of focal adhesions (vinculin, green) in control (A) and ΔItgα5/αv vSMCs (B) plated on Matrigel for 24hrs. Note the more rounded morphology and lack of cellular protrusions in α5/αv-deficient vSMCs. (C) Cell shape analysis of control, ΔItgαv, ΔItgα5 and ΔItgα5/αv vSMCs. An increased shape factor of ΔItgα5/αv vSMCs indicates a less complex and rounded cell shape. (D-E) Focal adhesion organisation in the lamellipodia of control (D) and ΔItgα5/αv vSMCs (E) as seen by immunofluorescence for phospho-FAK (red) and paxillin (green). ΔItgα5/αv vSMCs form only nascent adhesions and focal contacts whereas control cells form large focal adhesions. (F) Western blots showing that ΔItgα5/αv vSMCs have reduced levels of phosphorylation of FAK, paxillin and p130Cas. These reduced levels are rescued by re-expression of either α5 (ΔItgαv) or αv integrin (ΔItgα5). Scale bars: 10 μm (A, B, D, E).

Figure 7. TGF-β activation is mediated via α5 and αv integrins.
(A) Western blot showing that phosphorylation of SMAD2, but not of SMAD1/5/8, is reduced in ΔItgα5/αv vSMCs plated on Matrigel. (B) Immunofluorescence staining showing the level of pSMAD2 expression in the carotid arteries of control and *Itga5/av*$^{SM22\text{-}cre}$ embryos at E17.5. Note that pSMAD2 levels are increased within the dilated right carotid artery (RCA) as compared with the left carotid artery (LCA) of the mutant embryos. (C) Cell adhesion to the LAP of TGF-β1 is inhibited in ΔItgα5/αv cells. Adherent cells determined by absorbance of bound Crystal Violet. (D) ΔItgα5/αv cells are less able to assemble fibronectin (green) into fibrils or incorporate fibronectin, fibrillin-1, or fibulin-5 into the DOC-insoluble matrix (E). Note that despite the loss of fibrillin-1 and fibulin-5 assembly, elastin is still incorporated into the matrix by ΔItgα5/αv cells (E). (F) Incorporation of LTBP1, but not of LTBP3, into the DOC-insoluble matrix is inhibited by the loss of α5 and αv integrins. Scale bars: 50 μm (B), 20 μm (D).

Supplementary Materials and Methods

Histology and immunofluorescence staining

Freshly isolated embryos were embedded in Tissue-Tek OCT and sectioned (20μm) on a Cryostat; or fixed in 4% paraformaldehyde (PFA) in PBS at 4°C overnight or in zinc fixative (BD) at room temperature (RT) for 48 hours, followed by embedding and sectioning (5μm) in paraffin. Selected paraffin sections were stained with hematoxylin and eosin (H&E) using standard protocols.

For immunofluorescence staining, deparaffinized tissue sections were subjected to heat-induced epitope retrieval (2x5min 800W microwave) in 10 mM Tris Base, 1 mM EDTA Solution, 0.05% Tween 20, pH 9.0, blocked in PBS containing 0.5% Tween (PBS-T) and 2% goat, donkey or fibronectin-depleted goat serum and incubated overnight at 4°C with primary antibodies diluted in 1:1 PBS:PBS-T. After washes in PBS, tissues were incubated either at RT for 2 hours, or overnight at 4°C, with fluorophore-conjugated secondary antibodies diluted in 1:1 PBS-T. Samples were then washed in PBS, mounted onto coverslips in Fluoromount (Southern Biotech) and imaged using Zeiss LSM 510 or Nikon A1R scanning laser confocal microscopes. All images were processed using Volocity (Perkin Elmer) or Nikon Elements software. For whole-mount stainings, embryonic back skin from PFA-fixed embryos was removed and stained following the methods previously described in Foo et al. (2006). Staining for β-galactosidase (LacZ) activity; whole embryos or organs were dissected, fixed in 0.2% glutaraldehyde, 5mM EGTA, 2mM $MgCl_2$ in PBS for 15min at RT and stained following methods previously described in Nagy (2003).

vSMC isolation and culture

The aorta was dissected and all extra tissue and adventitia removed. The aorta was then cut into 2mm pieces and placed in collagenase type II for 4hrs at 37˚C, 5% CO_2. Digestion was stopped by the addition of fresh culture medium (DMEM containing 10% fetal calf serum, 2mM L-glutamine), centrifugation, and resuspension in fresh medium. The cells were then transferred to a single well of a 48-well plate and left undisturbed for 5 days at 37˚C, 5% CO_2.

Immunofluorescence staining of cells

For immunofluorescence experiments, cells were plated onto glass coverslips coated with Matrigel (20ug/ml), and fixed with 4% PFA or ice-cold methanol (for integrin αv staining). The cells were then permeabilised with 0.1% Triton X-100, blocked for 1h at room temperature in PBS containing 2% BSA, and incubated with primary antibodies diluted in blocking solution overnight at 4°C. After washing, cells were incubated with fluorophore-conjugated secondary antibodies at room temperature for 1h, washed, and mounted onto glass slides in Fluoromount.

Antibodies

Rat anti-mouse PECAM-1 MEC13.3, rat anti-mouse Integrin-α5 (BD Pharmingen), mouse anti-human αSMA Clone1A4-Cy3, mouse anti-Vinculin, mouse anti-Vimentin (Sigma), goat anti-GFP, rabbit anti-Fibulin-5, rabbit anti-Elastin, rabbit anti-Fibronectin, rabbit anti-Collagen IV, rabbit anti-Fibrillin-1, rabbit anti-Paxillin, rabbit anti-Myh11, rabbit anti-

SM22α (Abcam), Rabbit anti-FAK, rabbit anti-pFAK (pTyr397), rabbit anti-p130Cas (Y165), rabbit anti-pCRKL (Y207), rabbit anti-pSMAD2, rabbit anti-SMAD2, rabbit anti-SMAD1 (Cell Signaling), Rabbit anti-LTBP-1 (Abgent), Goat anti-Smoothelin, rabbit anti-LTBP-3 (Santa Cruz), mouse anti-GAPDH, Rabbit anti-Itgαv, rabbit anti-Itgα5, rabbit anti-pSMAD1/5/8 (Millipore).
Secondary antibodies were Alexa488, Alexa594, and Alexa647 conjugated antibodies (Invitrogen).

Immunoblotting

Novex Tris-glycine precast gels (Invitrogen) were used and wet-transferred to nitrocellulose. Blots were blocked and incubated with antibodies in 5% non-fat dried milk, 0.2% NP40, Tris-buffered saline (pH 8). Primary antibodies were integrin α5 (AB1928), αv (AB1930) and GAPDH (MAB374) (all from Millipore), vimentin (Sigma), and rabbit anti-fibronectin (297.1; generated in our laboratory). HRP-conjugated secondary antibodies were from Jackson ImmunoResearch: goat anti-rabbit and sheep anti-mouse IgM and HRP-streptavidin. Blots were developed using Western-Lightning ECL (PerkinElmer).

Real-time RT-PCR

RNA was isolated from cells using the RNAeasy kit (Qiagen) following the manufacturers' guidelines. cDNA synthesis was achieved by mixing 1μg of total RNA with 100pmole random hexamer primers and the Reverse Transcription System kit (Promega). Real-time RT-PCR was carried out using 5ng of cDNA, 300nmoles of each primer (see below) and 12.5μl of IQ SYBR green Supermix (Bio-Rad).

Gene	Forward Primer	Reverse Primer
Eln	GGCTTTGGACTTTCTCCCATT	CCGGCCACAGGATTTCC
Fn1	CTTTGGCAGTGGTCATTTCAG	ATTCTCCCTTTCCATTCCCG
Hspg2	TACGCGGTCCATTGAG	AGATCCGTCCGCATTC
Nd1	AACAATAGACACCAGTGCTCC	TCCCTTCACCTTGCCATTG
Fbn1	AATGAAGGCTATGAGGTGGC	TCTGTAGACTATACCCAGGCG
Col1a1	CATAAAGGGTCATCGTGGCT	TTGAGTCCGTCTTTGCCAG
Fbln4	AGCTACACGGAATGCACAG	AGGCAGACACAAATAACCCC
Fga	GAGAAAGCGCAACAGATTCAAG	TTATCTCACGGTTTACAGCCC
Lamb1	GGCAAACTGCAAAGTCTCG	CTGGAGGTGTTCCACAGGTC
Fbln5	ATGTCGCTATGGTTACTGCC	GGTCTGAACACAGGGATTCTC
Cola4a1	AGACCATTCAGATTCCGCAG	CGCTTCTAAACTCTTCCAGACAG
Vtn	CTACCGAGTCAACCTTAGAACC	GAAAGAGATGAGGCTCCTGAAG
tgfb1	CCTGAGTGGCTGTCTTTTGA	CGTGGAGTTTGTTATCTTTGCTG
Itga1	CCAACTCCAGTACATACCTGC	CTCCCACTTTATAGCTCCATT
Itga2	CGATACACATAACCCTCAGCTC	CTGCCTATGATAACCCCTGTC
Itga4	ATAAAGGCAAAGAGGTCCCAG	CGTCAGAAGTCCCATTAGAGAAG
Itga5	TGGAAGTCAGAAAGAGAATGGAG	GGTTCTTAGAATCCGAGACTGG
Itga6	GAGAGGCTTACTTCCGATGC	CCATGTGTTTCTCATCTTTGATCTC
Itga8	CATTGCTGTTCATCTTGCCC	CAGTAAAGACAACCCCAGAGG
Itga9	ATGAAGATGGTTGGGACTGG	ACAAAGATCAAGGACCACAGG
Itga10	CATCCCAACCCTCATCCTTC	AAGCCCCGAAGAGTAAATGG
Itga11	CTATGAGTGACCCAGAGTTGTG	CTGCTTTCTGATGTTTGGAAGG
Itgav	ACAGATGCAGTGTGAGGAAC	AAATGGTGATGGGAGTGAGC
Itgb1	TCCTATTTACAAGAGTGCCGTG	CCCTACTGTGACTAAGATGCTG
Itgb2	CAAACACAACGTGGCTTACAG	ACAATTCTTAGGGCTCTGCG
Itgb3	CAGTACTACGAAGACACCAGTG	CCAGATGAGCAGAGTAGCAGG
Itgb4	AGTGGGTAGAGGTGATACAAGG	TTAAGTGCAGAACAAAAGGCTG
Itgb5	TTCAGCTACACAGAACTGCC	GAGTGCCATCCCAATCAGG
Itgb6	AGTCACCCAAGAACAAGTCC	CTTCCAGTTCCACCTCAGAC
Itgb7	TCACAACCACTGTCAACCC	TCTTTGCCTGACAGACGC
Itgb8	TGAAGAGTGTGCCATGAAGAC	GCTACAACACTAGTCTCCAACAG

Supplementary Figure 1. Confirmation of vascular smooth muscle cell-specific expression of the *SM22α-Cre* recombinase.
(A) *SM22α–Cre*-mediated activation of the mTmG reporter, in which Cre-mediated excision results in the expression of membrane-bound GFP, in vascular smooth muscles (GFP, green), but not endothelial cells (red, PECAM-1) in the embryonic skin at E17.5. Scale bar: 50 μm.

Supplementary Figure 2. Survival numbers of *Itga5*$^{SM22\text{-}Cre}$, *Itgav*$^{SM22\text{-}Cre}$ and *Itga5/av*$^{SM22\text{-}Cre}$ mutant mice.
Table showing the number of live mutant mice, collected at the indicated developmental times. Percentages of live mice, as compared to controls (*Itga5*$^{flox/-}$; *Itgav*$^{flox/-}$), are shown in parentheses.

Supplementary Figure 3. Normal blood vessel morphology in vasculature of the skin.
Freshly isolated E17.5 control and *Itga5/av*$^{SM22\text{-}Cre}$ embryos. Note absence of obvious vascular defects.

Supplementary Figure 4. Normal neural crest distribution in *Itga5/av*$^{Wnt1\text{-}Cre}$ mutant mice.
Whole-mount Xgal-stained (blue) control (A) and *Itga5/av*$^{Wnt1\text{-}Cre}$ mutants (B) containing the Rosa26LacZ Cre reporter (Rosa26R) at indicated ages. Note *Wnt1*-positive neural crest cells in the aortic sac/outflow tract and III and IV pharyngeal arch arteries in both control and mutant embryos (enlarged images in insets). Sequential frontal sections through the outflow tract (OFT) of Rosa26R Cre reporter stained with Xgal (blue) in control (C) and *Itga5/av*$^{Wnt1\text{-}Cre}$ mutant (D) at E11.5. Note that the cushions of the OFT are already starting to septate the vessel into the pulmonary artery and aorta in control (indicated with an asterisks C).

Supplementary Figure 5. Survival numbers of *Itga5*$^{Wnt1\text{-}Cre}$, *Itgav*$^{Wnt1\text{-}Cre}$ and *Itga5/av*$^{Wnt1\text{-}Cre}$ mutant mice.
Table showing the number of live neural crest-specific mutants, collected at indicated developmental times. Percentage of live embryos or mice , as compared to controls (*Itga5*$^{flox/-}$; *Itgav*$^{flox/-}$), shown in parentheses.

Supplementary Figure 6. Normal vSMC differentiation in *Itga5/av*$^{SM22\text{-}Cre}$ mice.
(A) Frontal section through the brachiocephalic artery showing expression of αSMA (red) and Myh11 (green) in control and *Itga5/av*$^{SM22\text{-}Cre}$ embryos at E11.5. (B-D) Immunofluorescence stained transverse sections from E17.5 embryos confirming both control and *Itga5/av*$^{SM22\text{-}Cre}$ mice maintain expression of αSMA (B), SM22α (C), and Myh11 (D) in their neural-crest-derived vSMCs. Scale bars: 50 μm (A-D).

Supplementary Figure 7. No obvious proliferation defects within the vessel wall of *Itga5/av*$^{SM22\text{-}Cre}$ mice.
Frontal section through the brachiocephalic artery showing expression of αSMA (red) and Ki67 (green) in control and *Itga5/av*$^{SM22\text{-}Cre}$ embryos at E11.5. Scale bars: 100 μm.

Supplementary Figure 8. No obvious defects in the assembly of Fibronectin within the vessel wall of *Itga5/av*$^{SM22\text{-}Cre}$ mice.
Frontal sections through the right carotid artery of an E12.5 control and *Itga5/av*$^{SM22\text{-}Cre}$ embryo immunostained with anti-fibronectin antibody (green). Note the lack of any obvious defects in the assembly of fibronectin in the *Itga5/av*$^{SM22\text{-}Cre}$ embryo, notwithstanding dilation of the vessel. Scale bars: 50 μm.

Supplementary Figure 9. Characterisation of ΔItgα5/αv vSMCs.
(A) Cell adhesion assay showing that ΔItgα5/αv vSMCs have decreased adherence to collagen I and laminin. (B) Expression of integrins in ΔItgα5/αv vSMCs as compared to control cells. (C) Quantification of western blots from Fig. 6F. (D) Real-time RT-PCR showing somewhat elevated Tgfβ1 expression in ΔItgα5/αv cells plated on Matrigel at both sparse or confluent conditions normalised to control cells.

Supplementary Figure 10. TGF-β signalling in E12.5 embryos.
Frontal section through the brachiocephalic/carotid artery showing expression of αSMA (red) and pSMAD2 (green) in control and *Itga5/av*$^{SM22\text{-}Cre}$ embryos at E12.5). Scale bars: 50 μm.

Supplementary Figure 11. Expression and assembly of ECM proteins by ΔItgα5/αv vSMCs.
(A) ECM expression by ΔItgα5/αv vSMCs normalised to control cells. (B) DOC-insolubility assay showing that ΔItgα5/αv vSMCs cannot incorporate exogenous biotin-labelled fibronectin into the matrix over 5 days in culture.

References

Abraham, S., Kogata, N., Fassler, R. and Adams, R. H. (2008) 'Integrin beta1 subunit controls mural cell adhesion, spreading, and blood vessel wall stability', *Circ Res* 102(5): 562-70.

Alfandari, D., Cousin, H., Gaultier, A., Hoffstrom, B. G. and DeSimone, D. W. (2003) 'Integrin alpha5beta1 supports the migration of Xenopus cranial neural crest on fibronectin', *Dev Biol* 260(2): 449-64.

Annes, J. P., Rifkin, D. B. and Munger, J. S. (2002) 'The integrin alphaVbeta6 binds and activates latent TGFbeta3', *FEBS Lett* 511(1-3): 65-8.

Astrof, S. and Hynes, R. O. (2009) 'Fibronectins in vascular morphogenesis', *Angiogenesis* 12(2): 165-75.

Bader, B. L., Rayburn, H., Crowley, D. and Hynes, R. O. (1998) 'Extensive vasculogenesis, angiogenesis, and organogenesis precede lethality in mice lacking all alpha v integrins', *Cell* 95(4): 507-19.

Barillari, G., Albonici, L., Incerpi, S., Bogetto, L., Pistritto, G., Volpi, A., Ensoli, B. and Manzari, V. (2001) 'Inflammatory cytokines stimulate vascular smooth muscle cells locomotion and growth by enhancing alpha5beta1 integrin expression and function', *Atherosclerosis* 154(2): 377-85.

Bergwerff, M., Verberne, M. E., DeRuiter, M. C., Poelmann, R. E. and Gittenberger-de Groot, A. C. (1998) 'Neural crest cell contribution to the developing circulatory system: implications for vascular morphology?', *Circ Res* 82(2): 221-31.

Bruneau, B. G. (2008) 'The developmental genetics of congenital heart disease', *Nature* 451(7181): 943-8.

Cheng, Z., Sundberg-Smith, L. J., Mangiante, L. E., Sayers, R. L., Hakim, Z. S., Musunuri, S., Maguire, C. T., Majesky, M. W., Zhou, Z., Mack, C. P. et al. (2011) 'Focal adhesion kinase regulates smooth muscle cell recruitment to the developing vasculature', *Arterioscler Thromb Vasc Biol* 31(10): 2193-202.

Cheuk, B. L. and Cheng, S. W. (2004) 'Differential expression of integrin alpha5beta1 in human abdominal aortic aneurysm and healthy aortic tissues and its significance in pathogenesis', *J Surg Res* 118(2): 176-82.

Choudhary, B., Zhou, J., Li, P., Thomas, S., Kaartinen, V. and Sucov, H. M. (2009) 'Absence of TGFbeta signaling in embryonic vascular smooth muscle leads to reduced lysyl oxidase expression, impaired elastogenesis, and aneurysm', *Genesis* 47(2): 115-21.

Collins, C., Guilluy, C., Welch, C., O'Brien, E. T., Hahn, K., Superfine, R., Burridge, K. and Tzima, E. (2012) 'Localized tensional forces on PECAM-1 elicit a global mechanotransduction response via the integrin-RhoA pathway', *Curr Biol* 22(22): 2087-94.

D'Angelo, G., Mogford, J. E., Davis, G. E., Davis, M. J. and Meininger, G. A. (1997) 'Integrin-mediated reduction in vascular smooth muscle [Ca2+]i induced by RGD-containing peptide', *Am J Physiol* 272(4 Pt 2): H2065-70.

Dahm, L. M. and Bowers, C. W. (1998) 'Vitronectin regulates smooth muscle contractility via alphav and beta1 integrin', *J Cell Sci* 111 (Pt 9): 1175-83.

Danielian, P. S., Muccino, D., Rowitch, D. H., Michael, S. K. and McMahon, A. P. (1998) 'Modification of gene activity in mouse embryos in utero by a tamoxifen-inducible form of Cre recombinase', *Curr Biol* 8(24): 1323-6.

Davenpeck, K. L., Marcinkiewicz, C., Wang, D., Niculescu, R., Shi, Y., Martin, J. L. and Zalewski, A. (2001) 'Regional differences in integrin expression: role of alpha(5)beta(1) in regulating smooth muscle cell functions', *Circ Res* 88(3): 352-8.
Delannet, M., Martin, F., Bossy, B., Cheresh, D. A., Reichardt, L. F. and Duband, J. L. (1994) 'Specific roles of the alpha V beta 1, alpha V beta 3 and alpha V beta 5 integrins in avian neural crest cell adhesion and migration on vitronectin', *Development* 120(9): 2687-702.
El-Hamamsy, I. and Yacoub, M. H. (2009) 'Cellular and molecular mechanisms of thoracic aortic aneurysms', *Nat Rev Cardiol* 6(12): 771-86.
Flintoff-Dye, N. L., Welser, J., Rooney, J., Scowen, P., Tamowski, S., Hatton, W. and Burkin, D. J. (2005) 'Role for the alpha7beta1 integrin in vascular development and integrity', *Dev Dyn* 234(1): 11-21.
Foo, S. S., Turner, C. J., Adams, S., Compagni, A., Aubyn, D., Kogata, N., Lindblom, P., Shani, M., Zicha, D. and Adams, R. H. (2006) 'Ephrin-B2 controls cell motility and adhesion during blood-vessel-wall assembly', *Cell* 124(1): 161-73.
Francis, S. E., Goh, K. L., Hodivala-Dilke, K., Bader, B. L., Stark, M., Davidson, D. and Hynes, R. O. (2002) 'Central roles of alpha5beta1 integrin and fibronectin in vascular development in mouse embryos and embryoid bodies', *Arterioscler Thromb Vasc Biol* 22(6): 927-33.
Garmy-Susini, B., Jin, H., Zhu, Y., Sung, R. J., Hwang, R. and Varner, J. (2005) 'Integrin alpha4beta1-VCAM-1-mediated adhesion between endothelial and mural cells is required for blood vessel maturation', *J Clin Invest* 115(6): 1542-51.
George, E. L., Baldwin, H. S. and Hynes, R. O. (1997) 'Fibronectins are essential for heart and blood vessel morphogenesis but are dispensable for initial specification of precursor cells', *Blood* 90(8): 3073-81.
George, E. L., Georges-Labouesse, E. N., Patel-King, R. S., Rayburn, H. and Hynes, R. O. (1993) 'Defects in mesoderm, neural tube and vascular development in mouse embryos lacking fibronectin', *Development* 119(4): 1079-91.
Grazioli, A., Alves, C. S., Konstantopoulos, K. and Yang, J. T. (2006) 'Defective blood vessel development and pericyte/pvSMC distribution in alpha 4 integrin-deficient mouse embryos', *Dev Biol* 293(1): 165-77.
Hagel, M., George, E. L., Kim, A., Tamimi, R., Opitz, S. L., Turner, C. E., Imamoto, A. and Thomas, S. M. (2002) 'The adaptor protein paxillin is essential for normal development in the mouse and is a critical transducer of fibronectin signaling', *Mol Cell Biol* 22(3): 901-15.
Hakim, Z. S., DiMichele, L. A., Doherty, J. T., Homeister, J. W., Beggs, H. E., Reichardt, L. F., Schwartz, R. J., Brackhan, J., Smithies, O., Mack, C. P. et al. (2007) 'Conditional deletion of focal adhesion kinase leads to defects in ventricular septation and outflow tract alignment', *Mol Cell Biol* 27(15): 5352-64.
Hedin, U. and Thyberg, J. (1987) 'Plasma fibronectin promotes modulation of arterial smooth-muscle cells from contractile to synthetic phenotype', *Differentiation* 33(3): 239-46.
High, F. A., Zhang, M., Proweller, A., Tu, L., Parmacek, M. S., Pear, W. S. and Epstein, J. A. (2007) 'An essential role for Notch in neural crest during cardiovascular development and smooth muscle differentiation', *J Clin Invest* 117(2): 353-63.
Holtwick, R., Gotthardt, M., Skryabin, B., Steinmetz, M., Potthast, R., Zetsche, B., Hammer, R. E., Herz, J. and Kuhn, M. (2002) 'Smooth muscle-selective deletion of guanylyl cyclase-A prevents the acute but not chronic effects of ANP on blood pressure', *Proc Natl Acad Sci U S A* 99(10): 7142-7.

Horiguchi, M., Ota, M. and Rifkin, D. B. (2012) 'Matrix control of transforming growth factor-beta function', *J Biochem* 152(4): 321-9.
Huo, Y., Guo, X. and Kassab, G. S. (2008) 'The flow field along the entire length of mouse aorta and primary branches', *Ann Biomed Eng* 36(5): 685-99.
Hynes, R. O. (2007) 'Cell-matrix adhesion in vascular development', *J Thromb Haemost* 5 Suppl 1: 32-40.
Hynes, R. O. (2009) 'The extracellular matrix: not just pretty fibrils', *Science* 326(5957): 1216-9.
Ito, Y., Yeo, J. Y., Chytil, A., Han, J., Bringas, P., Jr., Nakajima, A., Shuler, C. F., Moses, H. L. and Chai, Y. (2003) 'Conditional inactivation of Tgfbr2 in cranial neural crest causes cleft palate and calvaria defects', *Development* 130(21): 5269-80.
Jiang, X., Rowitch, D. H., Soriano, P., McMahon, A. P. and Sucov, H. M. (2000) 'Fate of the mammalian cardiac neural crest', *Development* 127(8): 1607-16.
Keyte, A. and Hutson, M. R. (2012) 'The neural crest in cardiac congenital anomalies', *Differentiation* 84(1): 25-40.
Kirby, M. L., Gale, T. F. and Stewart, D. E. (1983) 'Neural crest cells contribute to normal aorticopulmonary septation', *Science* 220(4601): 1059-61.
Kirby, M. L. and Waldo, K. L. (1995) 'Neural crest and cardiovascular patterning', *Circ Res* 77(2): 211-5.
Lacy-Hulbert, A., Smith, A. M., Tissire, H., Barry, M., Crowley, D., Bronson, R. T., Roes, J. T., Savill, J. S. and Hynes, R. O. (2007) 'Ulcerative colitis and autoimmunity induced by loss of myeloid alphav integrins', *Proc Natl Acad Sci U S A* 104(40): 15823-8.
Li, J., Zhu, X., Chen, M., Cheng, L., Zhou, D., Lu, M. M., Du, K., Epstein, J. A. and Parmacek, M. S. (2005) 'Myocardin-related transcription factor B is required in cardiac neural crest for smooth muscle differentiation and cardiovascular development', *Proc Natl Acad Sci U S A* 102(25): 8916-21.
Liaw, L., Skinner, M. P., Raines, E. W., Ross, R., Cheresh, D. A., Schwartz, S. M. and Giachelli, C. M. (1995) 'The adhesive and migratory effects of osteopontin are mediated via distinct cell surface integrins. Role of alpha v beta 3 in smooth muscle cell migration to osteopontin in vitro', *J Clin Invest* 95(2): 713-24.
Lin, F. and Yang, X. (2010) 'TGF-beta signaling in aortic aneurysm: another round of controversy', *J Genet Genomics* 37(9): 583-91.
Ludbrook, S. B., Barry, S. T., Delves, C. J. and Horgan, C. M. (2003) 'The integrin alphavbeta3 is a receptor for the latency-associated peptides of transforming growth factors beta1 and beta3', *Biochem J* 369(Pt 2): 311-8.
Meng, H., Wang, Z., Hoi, Y., Gao, L., Metaxa, E., Swartz, D. D. and Kolega, J. (2007) 'Complex hemodynamics at the apex of an arterial bifurcation induces vascular remodeling resembling cerebral aneurysm initiation', *Stroke* 38(6): 1924-31.
Mikawa, T. and Gourdie, R. G. (1996) 'Pericardial mesoderm generates a population of coronary smooth muscle cells migrating into the heart along with ingrowth of the epicardial organ', *Dev Biol* 174(2): 221-32.
Mittal, A., Pulina, M., Hou, S. Y. and Astrof, S. (2010) 'Fibronectin and integrin alpha 5 play essential roles in the development of the cardiac neural crest', *Mech Dev* 127(9-12): 472-84.
Mittal, A., Pulina, M., Hou, S. Y. and Astrof, S. (2013) 'Fibronectin and integrin alpha 5 play requisite roles in cardiac morphogenesis', *Dev Biol* 381(1): 73-82.

Moiseeva, E. P. (2001) 'Adhesion receptors of vascular smooth muscle cells and their functions', *Cardiovasc Res* 52(3): 372-86.
Molin, D. G., Poelmann, R. E., DeRuiter, M. C., Azhar, M., Doetschman, T. and Gittenberger-de Groot, A. C. (2004) 'Transforming growth factor beta-SMAD2 signaling regulates aortic arch innervation and development', *Circ Res* 95(11): 1109-17.
Moustakas, A. and Heldin, C. H. (2005) 'Non-Smad TGF-beta signals', *J Cell Sci* 118(Pt 16): 3573-84.
Munger, J. S., Harpel, J. G., Giancotti, F. G. and Rifkin, D. B. (1998) 'Interactions between growth factors and integrins: latent forms of transforming growth factor-beta are ligands for the integrin alphavbeta1', *Mol Biol Cell* 9(9): 2627-38.
Munger, J. S., Huang, X., Kawakatsu, H., Griffiths, M. J., Dalton, S. L., Wu, J., Pittet, J. F., Kaminski, N., Garat, C., Matthay, M. A. et al. (1999) 'The integrin alpha v beta 6 binds and activates latent TGF beta 1: a mechanism for regulating pulmonary inflammation and fibrosis', *Cell* 96(3): 319-28.
Murphy, P. A. and Hynes, R. O. (2014) 'Alternative splicing of endothelial fibronectin is induced by disturbed hemodynamics and protects against hemorrhage of the vessel wall', *Arterioscler Thromb Vasc Biol* 34(9): 2042-50.
Muzumdar, M. D., Tasic, B., Miyamichi, K., Li, L. and Luo, L. (2007) 'A global double-fluorescent Cre reporter mouse', *Genesis* 45(9): 593-605.
Nagy, A. (2003) *Manipulating the mouse embryo : a laboratory manual*, Cold Spring Harbor, N.Y.: Cold Spring Harbor Laboratory Press.
Neubauer, K., Lindhorst, A., Tron, K., Ramadori, G. and Saile, B. (2008) 'Decrease of PECAM-1-gene-expression induced by proinflammatory cytokines IFN-gamma and IFN-alpha is reversed by TGF-beta in sinusoidal endothelial cells and hepatic mononuclear phagocytes', *BMC Physiol* 8: 9.
Panda, D., Kundu, G. C., Lee, B. I., Peri, A., Fohl, D., Chackalaparampil, I., Mukherjee, B. B., Li, X. D., Mukherjee, D. C., Seides, S. et al. (1997) 'Potential roles of osteopontin and alphaVbeta3 integrin in the development of coronary artery restenosis after angioplasty', *Proc Natl Acad Sci U S A* 94(17): 9308-13.
Papangeli, I. and Scambler, P. (2013) 'The 22q11 deletion: DiGeorge and velocardiofacial syndromes and the role of TBX1', *Wiley Interdiscip Rev Dev Biol* 2(3): 393-403.
Pera, J., Korostynski, M., Krzyszkowski, T., Czopek, J., Slowik, A., Dziedzic, T., Piechota, M., Stachura, K., Moskala, M., Przewlocki, R. et al. (2010) 'Gene expression profiles in human ruptured and unruptured intracranial aneurysms: what is the role of inflammation?', *Stroke* 41(2): 224-31.
Piali, L., Hammel, P., Uherek, C., Bachmann, F., Gisler, R. H., Dunon, D. and Imhof, B. A. (1995) 'CD31/PECAM-1 is a ligand for alpha v beta 3 integrin involved in adhesion of leukocytes to endothelium', *J Cell Biol* 130(2): 451-60.
Raines, E. W. (2000) 'The extracellular matrix can regulate vascular cell migration, proliferation, and survival: relationships to vascular disease', *Int J Exp Pathol* 81(3): 173-82.
Ray, J. L., Leach, R., Herbert, J. M. and Benson, M. (2001) 'Isolation of vascular smooth muscle cells from a single murine aorta', *Methods Cell Sci* 23(4): 185-8.
Rensen, S. S., Doevendans, P. A. and van Eys, G. J. (2007) 'Regulation and characteristics of vascular smooth muscle cell phenotypic diversity', *Neth Heart J* 15(3): 100-8.

Savolainen, S. M., Foley, J. F. and Elmore, S. A. (2009) 'Histology atlas of the developing mouse heart with emphasis on E11.5 to E18.5', *Toxicol Pathol* 37(4): 395-414.
Scheppke, L., Murphy, E. A., Zarpellon, A., Hofmann, J. J., Merkulova, A., Shields, D. J., Weis, S. M., Byzova, T. V., Ruggeri, Z. M., Iruela-Arispe, M. L. et al. (2012) 'Notch promotes vascular maturation by inducing integrin-mediated smooth muscle cell adhesion to the endothelial basement membrane', *Blood* 119(9): 2149-58.
Soriano, P. (1999) 'Generalized lacZ expression with the ROSA26 Cre reporter strain', *Nat Genet* 21(1): 70-1.
Takahashi, S., Leiss, M., Moser, M., Ohashi, T., Kitao, T., Heckmann, D., Pfeifer, A., Kessler, H., Takagi, J., Erickson, H. P. et al. (2007) 'The RGD motif in fibronectin is essential for development but dispensable for fibril assembly', *J Cell Biol* 178(1): 167-78.
ten Dijke, P. and Arthur, H. M. (2007) 'Extracellular control of TGFbeta signalling in vascular development and disease', *Nat Rev Mol Cell Biol* 8(11): 857-69.
Todorovic, V., Frendewey, D., Gutstein, D. E., Chen, Y., Freyer, L., Finnegan, E., Liu, F., Murphy, A., Valenzuela, D., Yancopoulos, G. et al. (2007) 'Long form of latent TGF-beta binding protein 1 (Ltbp1L) is essential for cardiac outflow tract septation and remodeling', *Development* 134(20): 3723-32.
Turlo, K. A., Noel, O. D., Vora, R., LaRussa, M., Fassler, R., Hall-Glenn, F. and Iruela-Arispe, M. L. (2012) 'An essential requirement for beta1 integrin in the assembly of extracellular matrix proteins within the vascular wall', *Dev Biol* 365(1): 23-35.
Turner, C. J., Badu-Nkansah, K., Crowley, D., van der Flier, A. and Hynes, R. O. (2014) 'Integrin-alpha5beta1 is not required for mural cell functions during development of blood vessels but is required for lymphatic-blood vessel separation and lymphovenous valve formation', *Dev Biol* 392(2): 381-92.
Vallejo-Illarramendi, A., Zang, K. and Reichardt, L. F. (2009) 'Focal adhesion kinase is required for neural crest cell morphogenesis during mouse cardiovascular development', *J Clin Invest* 119(8): 2218-30.
van der Flier, A., Badu-Nkansah, K., Whittaker, C. A., Crowley, D., Bronson, R. T., Lacy-Hulbert, A. and Hynes, R. O. (2010) 'Endothelial alpha5 and alphav integrins cooperate in remodeling of the vasculature during development', *Development* 137(14): 2439-49.
Veith, C., Marsh, L. M., Wygrecka, M., Rutschmann, K., Seeger, W., Weissmann, N. and Kwapiszewska, G. (2012) 'Paxillin regulates pulmonary arterial smooth muscle cell function in pulmonary hypertension', *Am J Pathol* 181(5): 1621-33.
Wagenseil, J. E. and Mecham, R. P. (2009) 'Vascular extracellular matrix and arterial mechanics', *Physiol Rev* 89(3): 957-89.
Waldo, K. L., Hutson, M. R., Ward, C. C., Zdanowicz, M., Stadt, H. A., Kumiski, D., Abu-Issa, R. and Kirby, M. L. (2005) 'Secondary heart field contributes myocardium and smooth muscle to the arterial pole of the developing heart', *Dev Biol* 281(1): 78-90.
Wang, J., Nagy, A., Larsson, J., Dudas, M., Sucov, H. M. and Kaartinen, V. (2006) 'Defective ALK5 signaling in the neural crest leads to increased postmigratory neural crest cell apoptosis and severe outflow tract defects', *BMC Dev Biol* 6: 51.
Wang, Y., Dur, O., Patrick, M. J., Tinney, J. P., Tobita, K., Keller, B. B. and Pekkan, K. (2009) 'Aortic arch morphogenesis and flow modeling in the chick embryo', *Ann Biomed Eng* 37(6): 1069-81.

Wasteson, P., Johansson, B. R., Jukkola, T., Breuer, S., Akyurek, L. M., Partanen, J. and Lindahl, P. (2008) 'Developmental origin of smooth muscle cells in the descending aorta in mice', *Development* 135(10): 1823-32.
Wu, X., Davis, G. E., Meininger, G. A., Wilson, E. and Davis, M. J. (2001) 'Regulation of the L-type calcium channel by alpha 5beta 1 integrin requires signaling between focal adhesion proteins', *J Biol Chem* 276(32): 30285-92.
Wurdak, H., Ittner, L. M., Lang, K. S., Leveen, P., Suter, U., Fischer, J. A., Karlsson, S., Born, W. and Sommer, L. (2005) 'Inactivation of TGFbeta signaling in neural crest stem cells leads to multiple defects reminiscent of DiGeorge syndrome', *Genes Dev* 19(5): 530-5.
Xie, W. B., Li, Z., Shi, N., Guo, X., Tang, J., Ju, W., Han, J., Liu, T., Bottinger, E. P., Chai, Y. et al. (2013) 'Smad2 and myocardin-related transcription factor B cooperatively regulate vascular smooth muscle differentiation from neural crest cells', *Circ Res* 113(8): e76-86.
Yang, J. T. and Hynes, R. O. (1996) 'Fibronectin receptor functions in embryonic cells deficient in alpha 5 beta 1 integrin can be replaced by alpha V integrins', *Mol Biol Cell* 7(11): 1737-48.
Yang, J. T., Rayburn, H. and Hynes, R. O. (1993) 'Embryonic mesodermal defects in alpha 5 integrin-deficient mice', *Development* 119(4): 1093-105.
Yang, M., Jiang, H. and Li, L. (2010) 'Sm22alpha transcription occurs at the early onset of the cardiovascular system and the intron 1 is dispensable for its transcription in smooth muscle cells during mouse development', *Int J Physiol Pathophysiol Pharmacol* 2(1): 12-9.
Yang, Z., Mu, Z., Dabovic, B., Jurukovski, V., Yu, D., Sung, J., Xiong, X. and Munger, J. S. (2007) 'Absence of integrin-mediated TGFbeta1 activation in vivo recapitulates the phenotype of TGFbeta1-null mice', *J Cell Biol* 176(6): 787-93.
Yashiro, K., Shiratori, H. and Hamada, H. (2007) 'Haemodynamics determined by a genetic programme govern asymmetric development of the aortic arch', *Nature* 450(7167): 285-8.
Zhao, J. J., Gjoerup, O. V., Subramanian, R. R., Cheng, Y., Chen, W., Roberts, T. M. and Hahn, W. C. (2003) 'Human mammary epithelial cell transformation through the activation of phosphatidylinositol 3-kinase', *Cancer Cell* 3(5): 483-95.
Zilberberg, L., Todorovic, V., Dabovic, B., Horiguchi, M., Courousse, T., Sakai, L. Y. and Rifkin, D. B. (2012) 'Specificity of latent TGF-beta binding protein (LTBP) incorporation into matrix: role of fibrillins and fibronectin', *J Cell Physiol* 227(12): 3828-36.

Figure 1

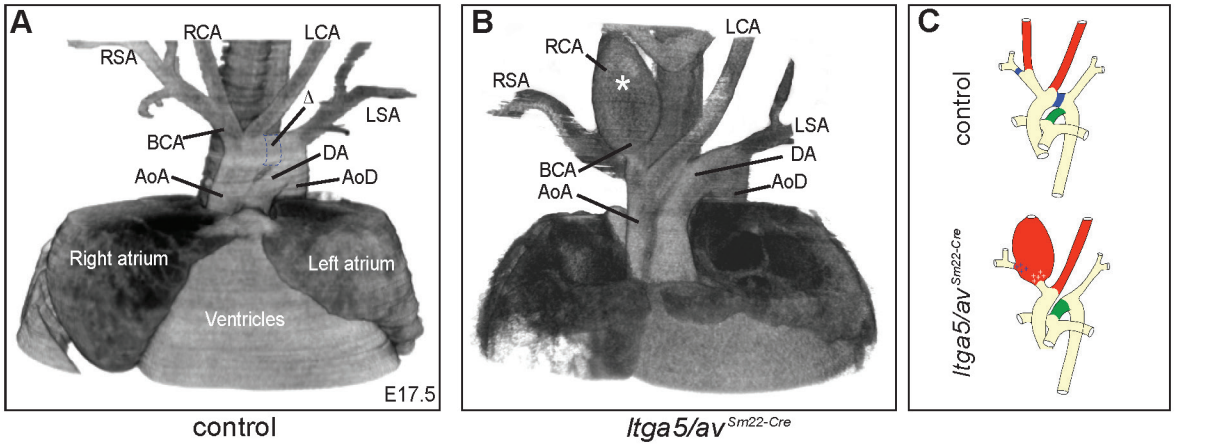
A
RCA
LCA
RSA
LSA
BCA
DA
AoA
AoD
Right atrium
Left atrium
Ventricles
E17.5
control
B
RCA
LCA
RSA
LSA
BCA
DA
AoA
AoD
Itga5/av Sm22-Cre
C
control
Itga5/av Sm22-Cre

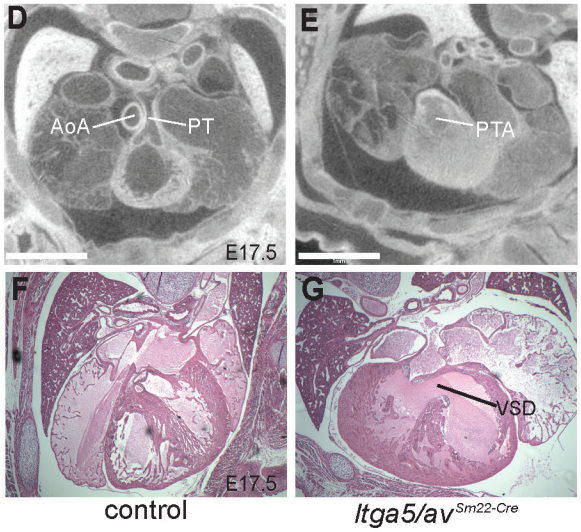
D
AoA
PT
E17.5
E
PTA
F
E17.5
control
G
VSD
Itga5/av Sm22-Cre

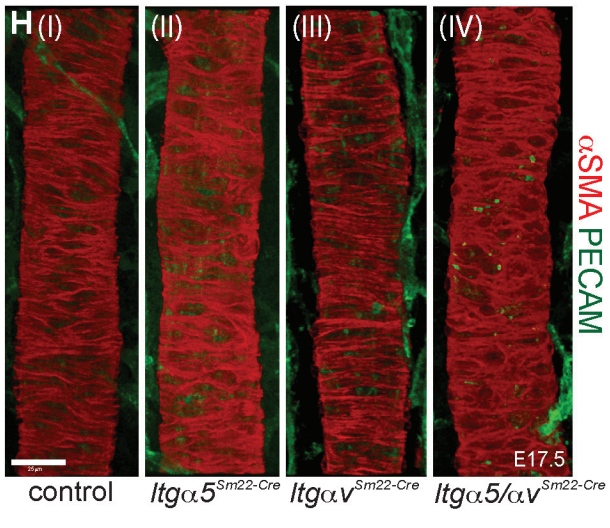
H (I)
(II)
(III)
(IV)
E17.5
αSMA PECAM
control
Itgα5 Sm22-Cre
Itgαv Sm22-Cre
Itgα5/αv Sm22-Cre

Figure 2

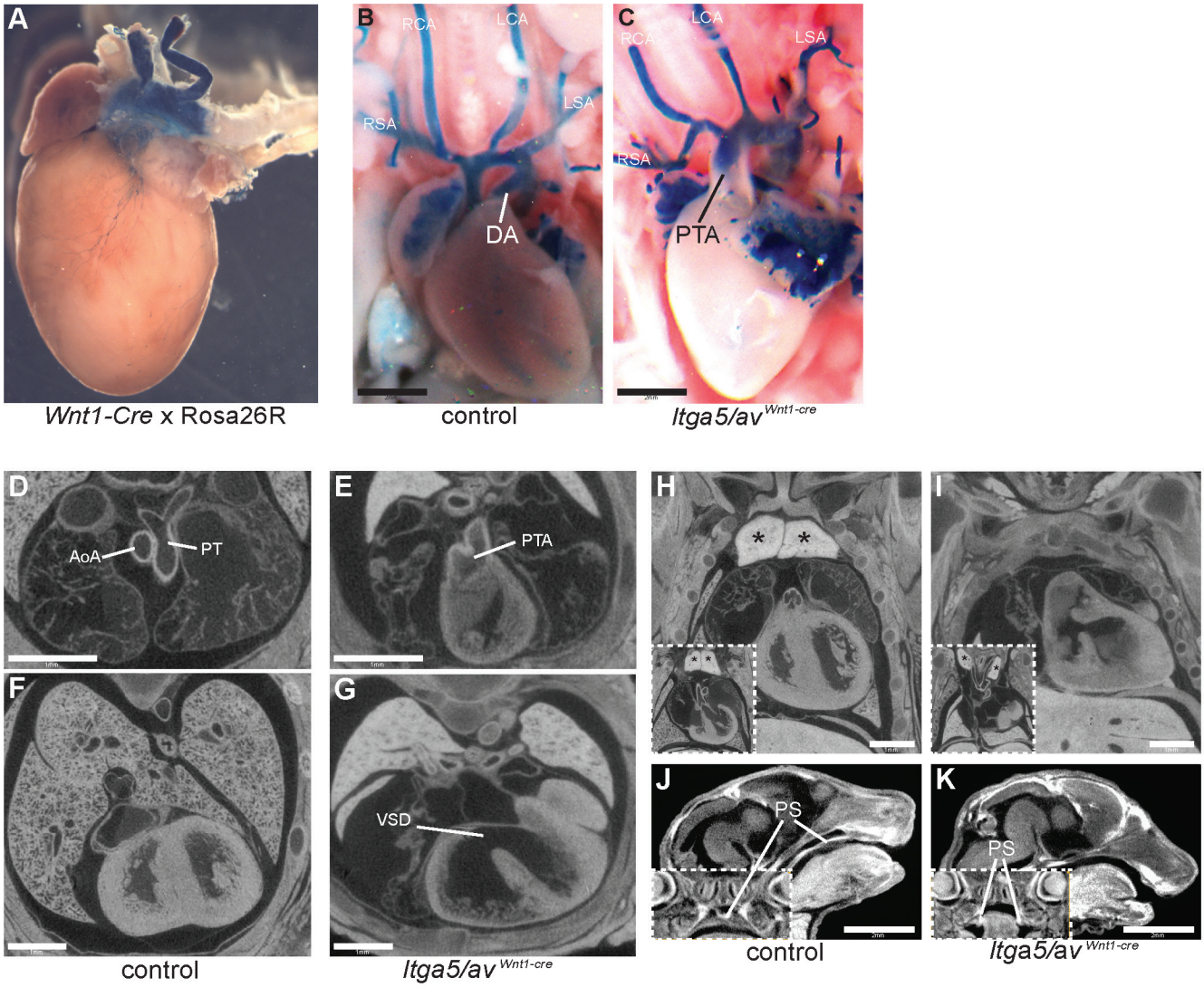
A
Wnt1-Cre x Rosa26R
B
RCA
LCA
LSA
RSA
DA
control
C
LCA
RCA
LSA
RSA
PTA
Itga5/av Wnt1-cre
D
AoA
PT
E
PTA
H
I
F
G
VSD
control
Itga5/av Wnt1-cre
J
PS
K
PS
control
Itga5/av Wnt1-cre

Figure 3

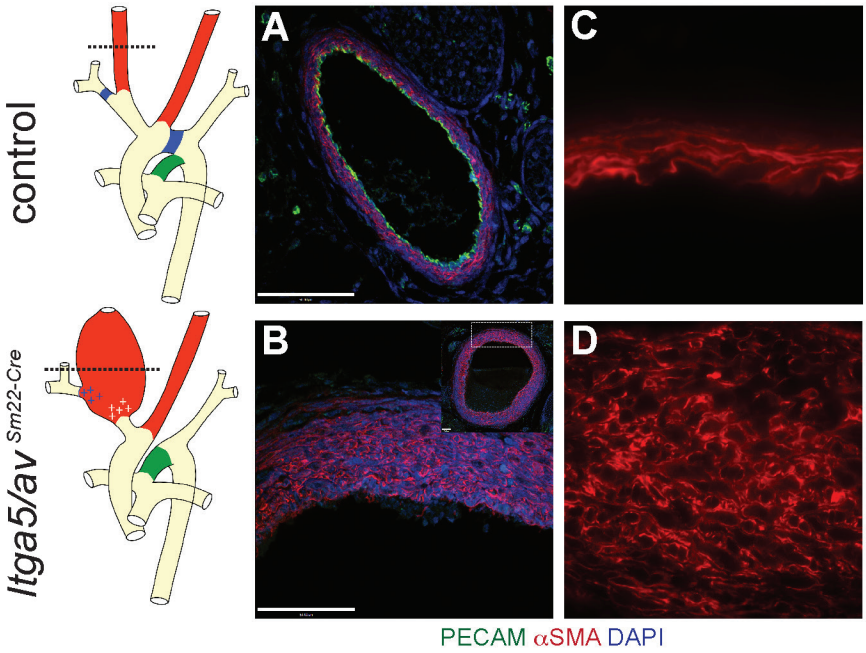

Figure 4

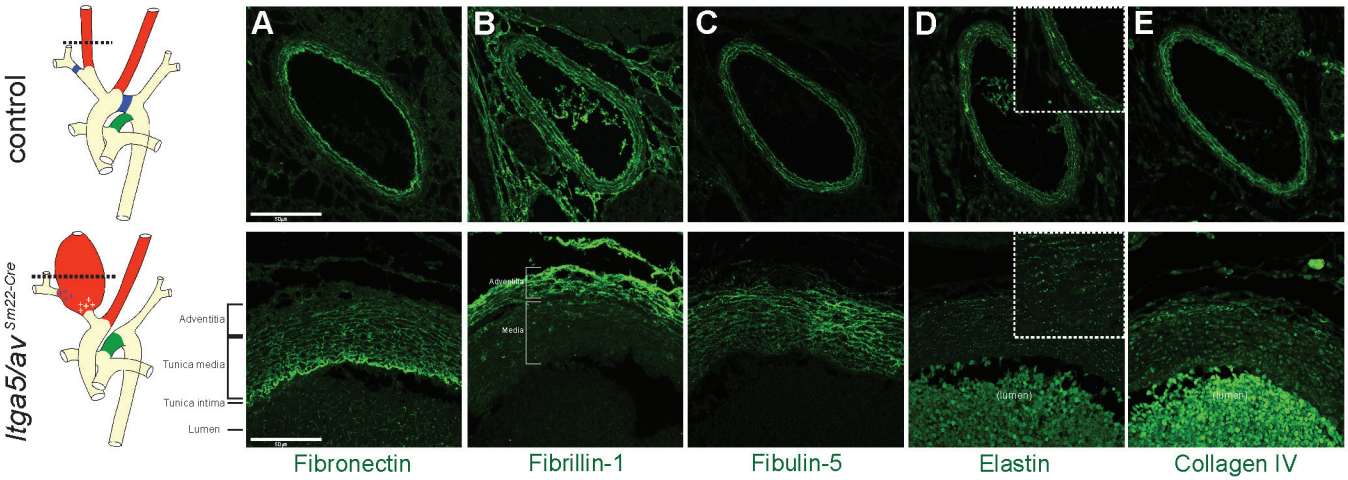
control
Itga5/av Sm22-Cre
A
B
C
D
E
Adventitia
Tunica media
Tunica intima
Lumen
Media
(lumen)
Fibronectin
Fibrillin-1
Fibulin-5
Elastin
Collagen IV

Figure 5

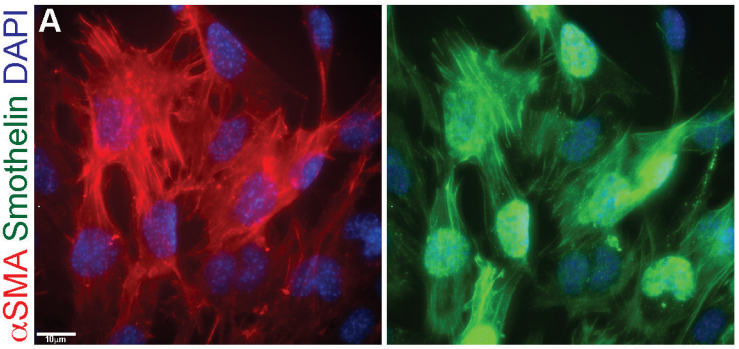
A
αSMA Smothelin DAPI
10μm

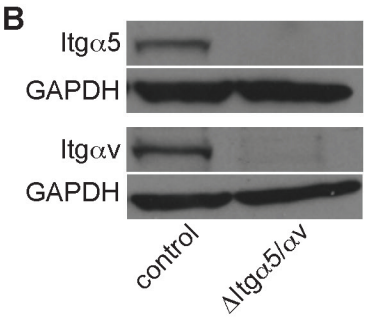
B
Itgα5
GAPDH
Itgαv
GAPDH
control
Δltgα5/αv

C

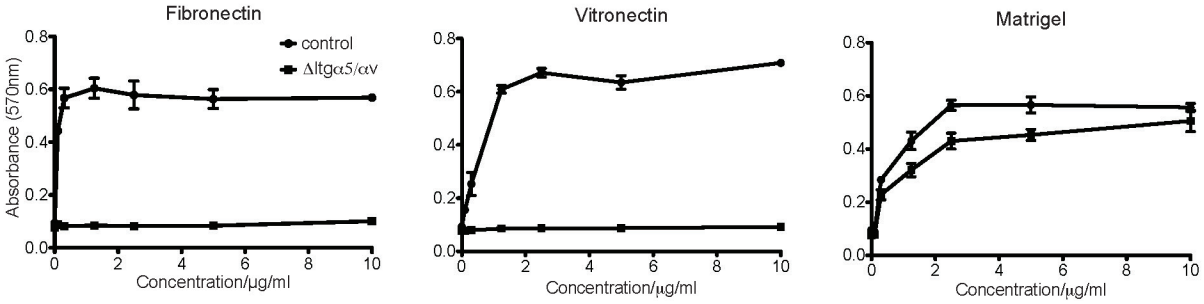
Fibronectin
control
Δltgα5/αv
Absorbance (570nm)
Concentration/μg/ml
Vitronectin
Concentration/μg/ml
Matrigel
Concentration/μg/ml

Figure 6

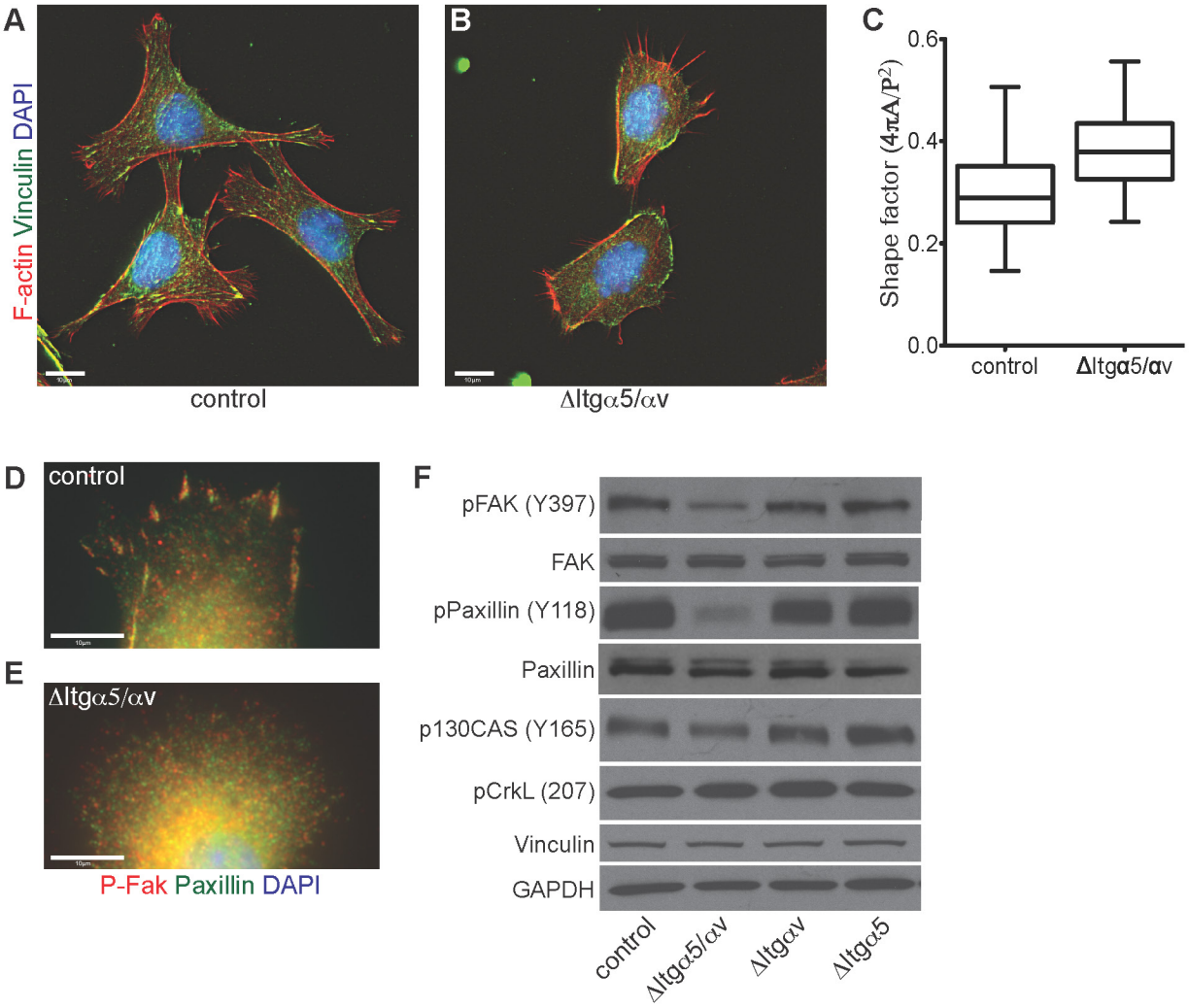
A
F-actin Vinculin DAPI
control
B
ΔItgα5/αv
C
Shape factor (4πA/P²)
0.6
0.4
0.2
0.0
control
ΔItgα5/αv
D
control
E
ΔItgα5/αv
P-Fak Paxillin DAPI
F
pFAK (Y397)
FAK
pPaxillin (Y118)
Paxillin
p130CAS (Y165)
pCrkL (207)
Vinculin
GAPDH
control
ΔItgα5/αv
ΔItgαv
ΔItgα5

Figure 7

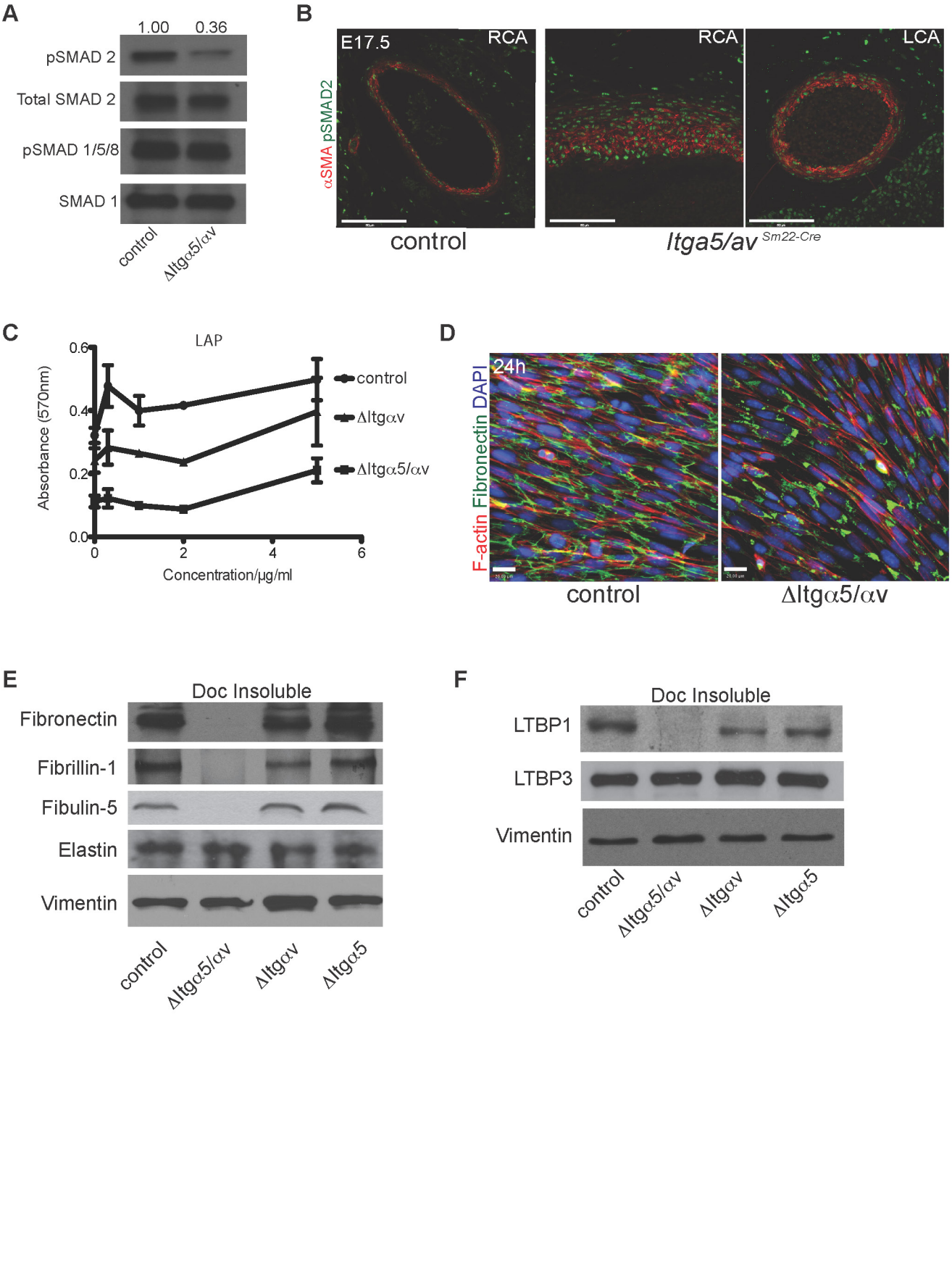
A
1.00
0.36
pSMAD 2
Total SMAD 2
pSMAD 1/5/8
SMAD 1
control
ΔItgα5/αv
B
E17.5
RCA
RCA
LCA
αSMA pSMAD2
control
Itga5/av Sm22-Cre
C
LAP
Absorbance (570nm)
0.6
0.4
0.2
0.0
0
2
4
6
Concentration/μg/ml
control
ΔItgαv
ΔItgα5/αv
D
24h
F-actin Fibronectin DAPI
control
ΔItgα5/αv
E
Doc Insoluble
Fibronectin
Fibrillin-1
Fibulin-5
Elastin
Vimentin
control
ΔItgα5/αv
ΔItgαv
ΔItgα5
F
Doc Insoluble
LTBP1
LTBP3
Vimentin
control
ΔItgα5/αv
ΔItgαv
ΔItgα5

Supplementary Figure 1

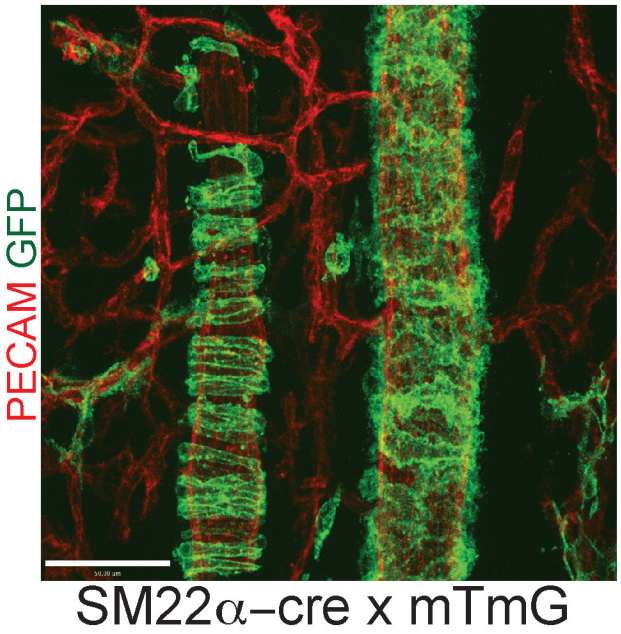

Supplementary Figure 2

Survival Numbers

	control	*Itgα5*$^{Sm22\text{-}cre}$	*Itgαv*$^{Sm22\text{-}cre}$	*Itgα5/αv*$^{Sm22\text{-}cre}$
E12.5	9	9 (100%)	10 (100%)	8 (89%)
E13.5	17	15 (88%)	22 (100%)	13 (76%)
E14.5	7	9 (100%)	9 (100%)	9 (100%)
E15.5	5	5 (100%)	5 (100%)	5 (100%)
E17.5	23	24 (100%)	26 (100%)	12 (52%)
P21	59	29 (49%)	23 (39%)	0 (0%)

Supplementary Figure 3

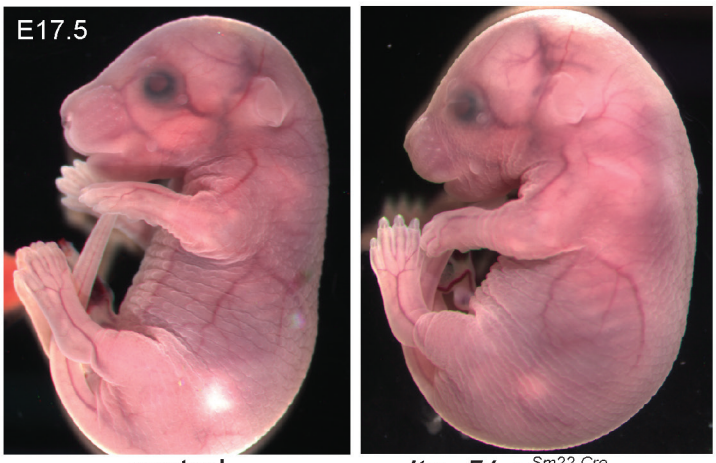

Supplementary Figure 4

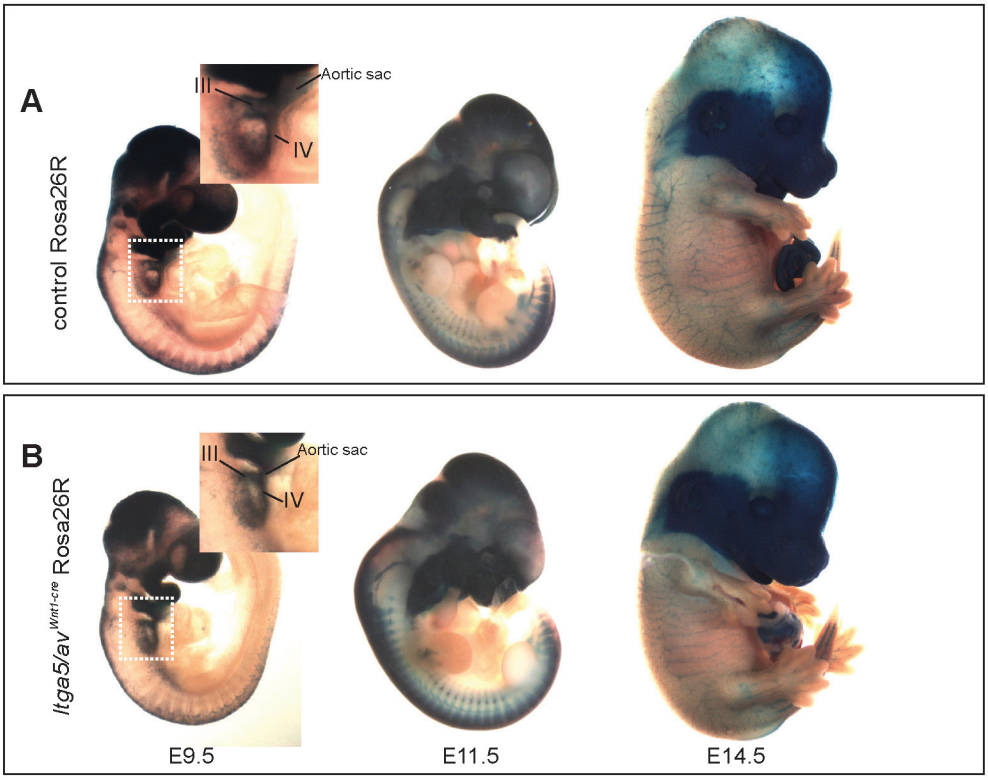

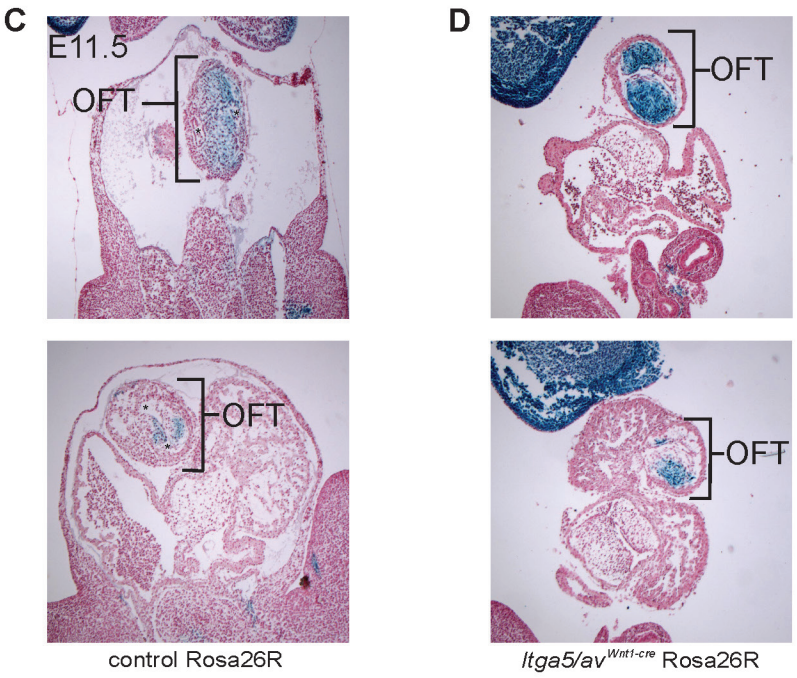

Supplementary Figure 5

Survival Numbers

	control	*Itgα5*$^{Wnt1\text{-}cre}$	*Itgαv*$^{Wnt1\text{-}cre}$	*Itgα5/αv*$^{Wnt1\text{-}cre}$
E10.5	3	3 (100%)	1 (33%)	5 (100%)
E11.5	8	9 (100%)	16 (100%)	14 (100%)
E15.5	6	5 (83%)	6 (100%)	5 (83%)
E17.5	24	24 (100%)	16 (67%)	12 (50%)
P21	22	0 (0%)	2 (9%)	0 (0%)

Supplementary Figure 6

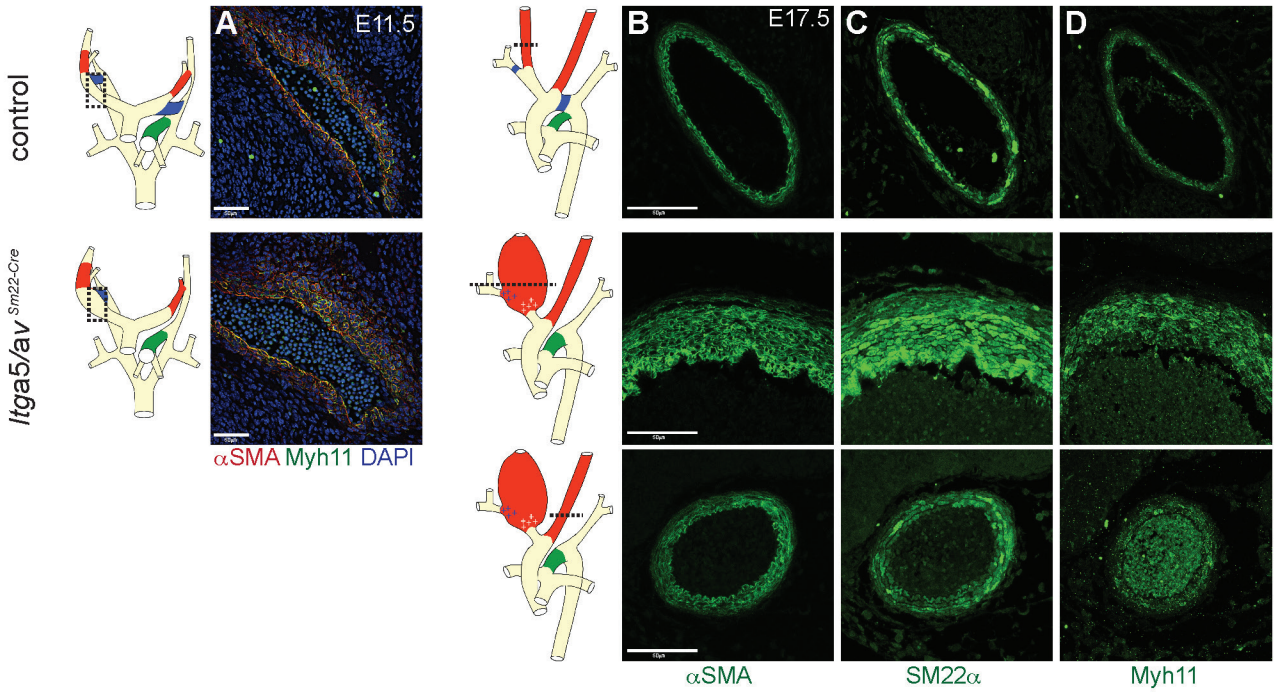

Supplementary Figure 7

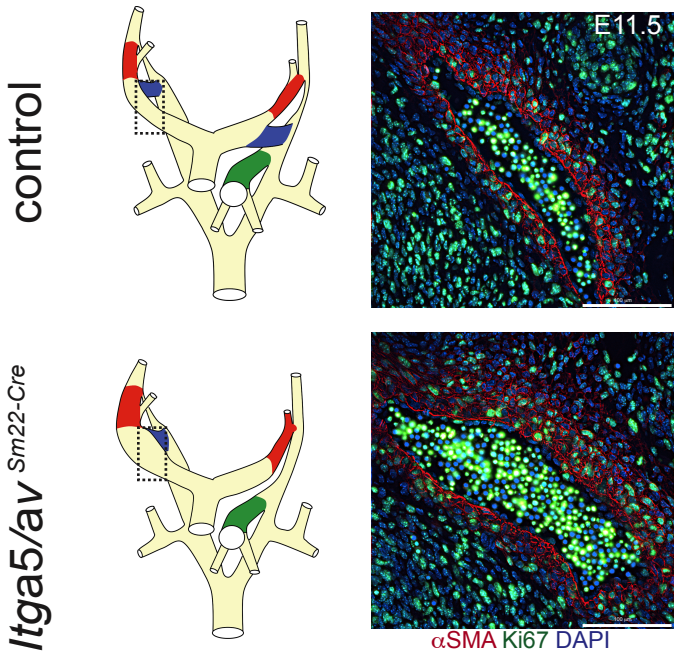

Supplementary Figure 8

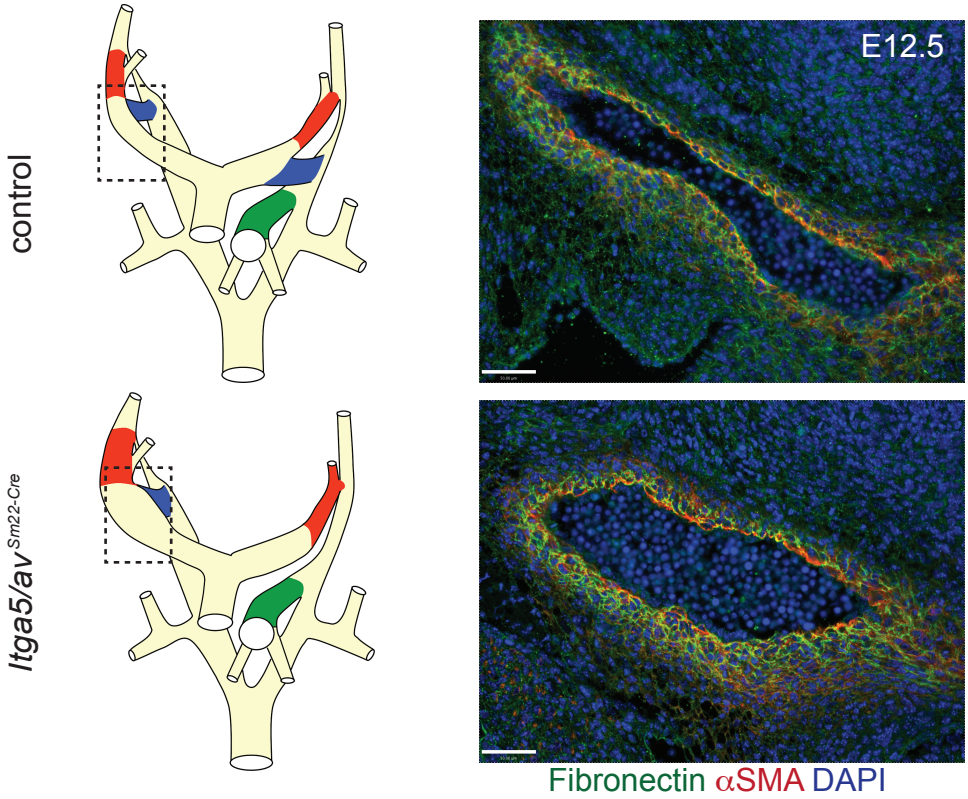

Supplementary Figure 9

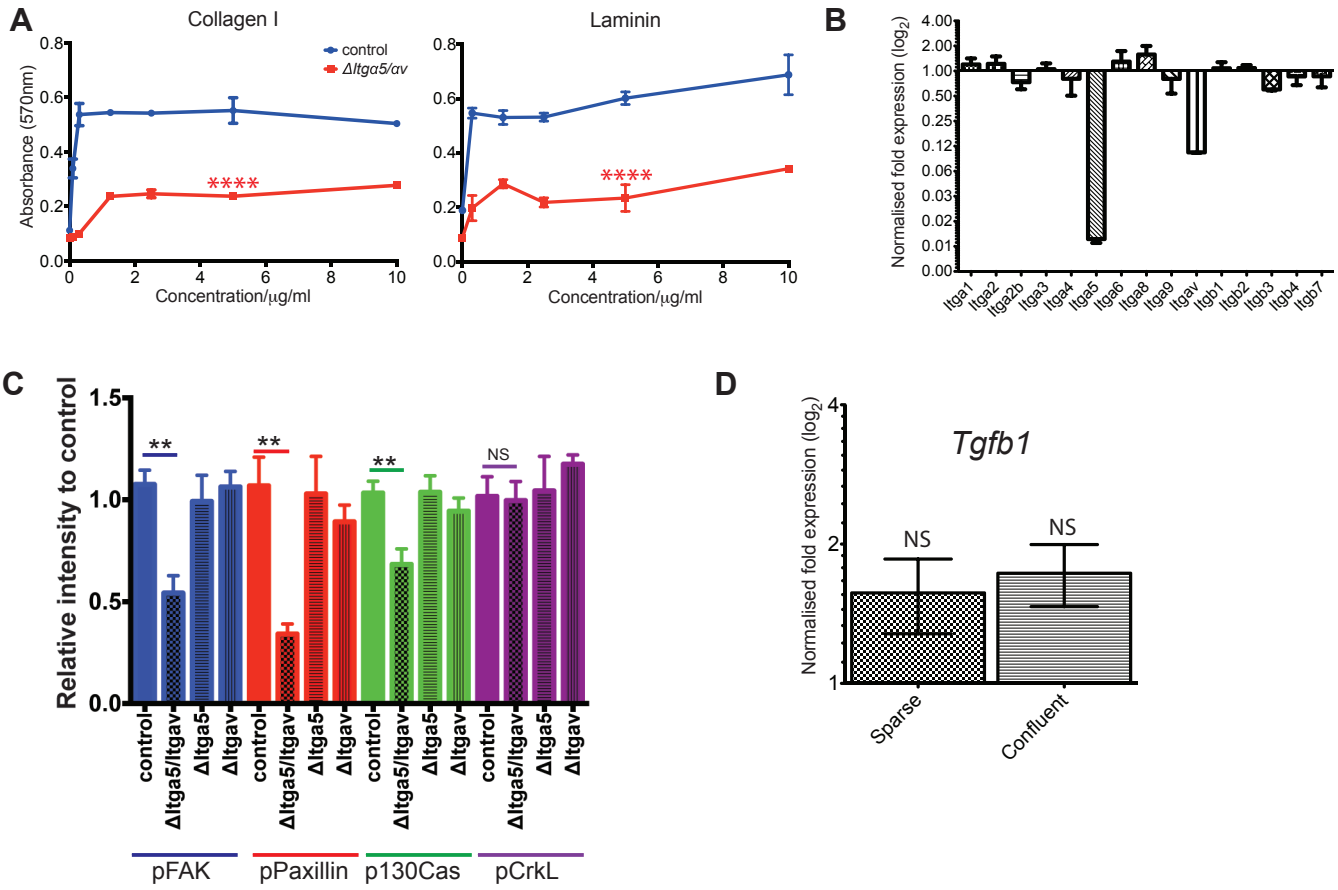

Supplementary Figure 10

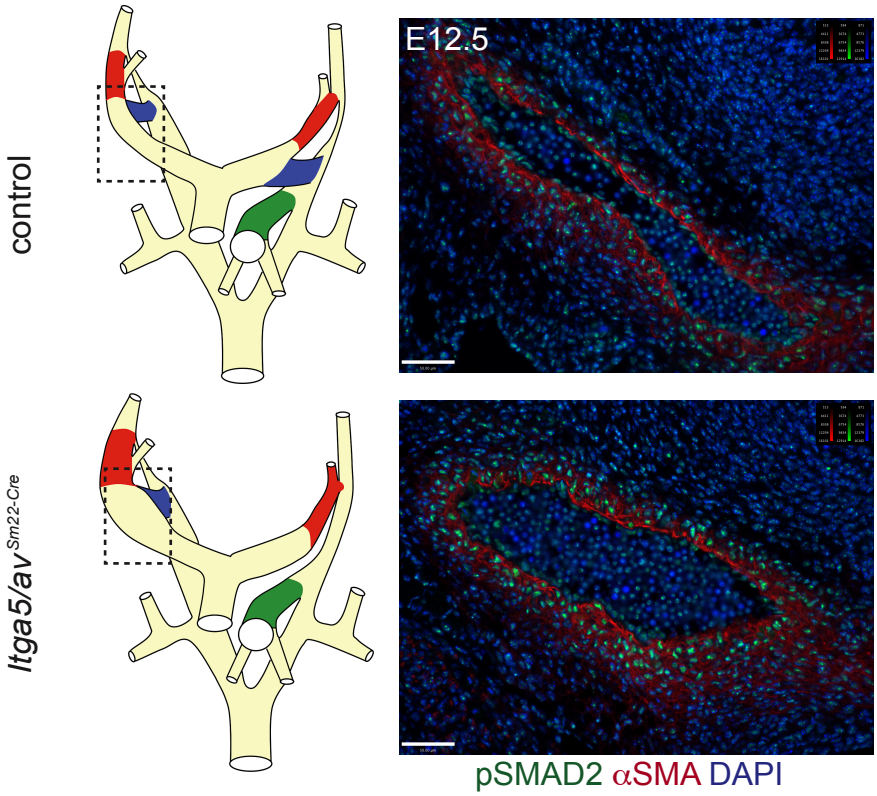

Supplementary Figure 11